NATIONAL ADVISORY COMMITTEE FOR AERONAUTICS

TECHNICAL NOTE 2618

CREEP IN METALS

By A. D. Schwope, F. R. Shober,
and L. R. Jackson

Battelle Memorial Institute

NACA

Washington
February 1952

NATIONAL ADVISORY COMMITTEE FOR AERONAUTICS

TECHNICAL NOTE 2618

CREEP IN METALS

By A. D. Schwope, F. R. Shober,
and L. R. Jackson

SUMMARY

This report covers initial phases of an investigation of the fundamental of creep in metals. Results of a study of creep in single crystals of high-purity aluminum are presented and discussed. It is shown that at low stresses the creep phenomenon appears to be consistent with Mott and Nabarro's theory of exhaustion creep while at higher stresses results appear to be more in accord with ideas expressed by Andrade.

INTRODUCTION

The investigation reported here was based on the idea that the development of an adequate theory of creep in metals is hampered by the lack of data taken under sufficiently definitive conditions. The objective of the work, then, was to attempt to obtain data of the type required and to show the extent to which these data do or do not agree with current theories of creep.

In order to limit the number of variables under consideration, the investigation so far has been confined to a study of creep of single crystals of high-purity aluminum as a function of stress at constant temperature. Aluminum was selected for these initial studies partly because it is more nearly isotropic than other metals and partly because a good deal of information could be obtained near room temperature so the experimental techniques could be simplified.

In order to conduct the investigation so as to provide sufficiently detailed information, the following steps were required:

(1) It was necessary to grow considerable numbers of large single crystals (this was done by the strain-anneal method)

(2) It was necessary to conduct tests to establish that the crystals were really single crystals and to determine the orientation of each crystal

(3) In order to provide a basis for relating creep to other mechanical properties and to obtain information required to use the creep data in various theories, it was necessary to determine the elastic modulus, the critical resolved shear stress, and other properties of the crystals

Throughout the investigation, every attempt was made to link every step with any previous work known. This was done so that the data obtained could be properly evaluated.

This investigation was conducted at the Battelle Memorial Institute under the sponsorship and with the financial assistance of the National Advisory Committee for Aeronautics.

PRODUCTION OF SINGLE CRYSTALS

Single crystals were grown by the strain-anneal method, which was advantageous because the desired size and shape of specimen can be machined prior to growth of the crystals. While it is possible to machine and shape single crystals of some metals, aluminum single crystals are very soft and would be greatly distorted by machining. It was imperative that uniform specimens be used in this work and for that reason the strain-anneal method was used.

This method was essentially an anneal-strain-anneal procedure. The first anneal was primarily to produce grains of uniform size and to relieve any strain that might have been induced during machining. The next step, straining, was accomplished by pulling the specimen in a tensile machine until an elongation of 0.5 to 1.5 percent was produced. Carpenter and Elam (reference 1) found that 99.95 percent aluminum grew into single crystals more frequently when the specimen had been elongated from 1.5 to 2 percent before annealing. However, it was found that less elongation, from 0.5 to 1.5 percent, is necessary to grow single crystals from the 99.99+ percent aluminum.

The final annealing temperature can only be found by trial and error, since it varies for different metals and different purities of the same metal. In general, the procedure was to put the strained specimen into a furnace at a temperature where there was no recrystallization or grain growth and gradually to increase the temperature. The annealing was finished at a temperature between 625° and 650° C to complete the absorption of small crystals that tend to remain at the surface.

The following summary of the strain-anneal method as used at the Aluminum Company of America (reference 2) was followed closely in this investigation:

(1) The specimens are machined to the desired shape and size from cold-rolled bar stock (for these experiments, standard 0.505-in. tensile bars were used)

(2) The specimens are annealed for 6 hours at 550° C

(3) The specimens are strained in tension to produce a permanent elongation of 0.5 to 2 percent in the gage length, depending on the purity of the aluminum used

(4) The specimens are then placed in a furnace, heated rapidly to 450° C and held at that temperature for 24 hours

(5) The temperature of the furnace is raised 20° C per day until 600° C is reached

(6) The specimen is held at the final anneal temperature, 635° to 650° C, for 48 hours

Establishing Perfection of Single Crystals

An intensive examination was carried out to determine the perfection of the crystals. It has been reported by Burke (reference 3) that it became increasingly difficult to grow single crystals of aluminum as the purity increased. Since in this investigation it was found that single crystals were easier to grow from the 99.99+ percent metal than from the 99.95 percent aluminum, there appeared to be some discrepancy in the facts. Accordingly, optical and electron microscopy utilizing the etch-pit techniques as well as ordinary polishing and etching procedures was employed. The results were negative in the sense that crystals whose boundaries were determined with a macroetchant could not be broken down to subgrains or macromosaics. Figures 1, 2, and 3 are Lauegrams taken at three different spots along the length of a 2-inch crystal. The photograms are identical, a verification that the specimen was a single crystal.

Determination of Orientation of Crystals

The orientations of the single crystals were determined by the Laue back-reflection X-ray technique. The procedure followed has been thoroughly described by Barrett (reference 4). The results for the crystals used in this portion of the investigation are given in table 1.

Letters A, B, C, and D are the poles of the four (111) slip planes and U, V, W, X, Y, and Z with the lettered subscripts refer to the [110] slip directions lying in the (111) planes. The angle between the normal to the slip plane and the specimen axis is given in the column headed ϕ. The angle between the slip direction and the specimen axis is designated as λ. It is observed that not all the planes or directions are listed. This is because the product $\cos \phi \cos \lambda$ was too small and that particular slip system had little chance of becoming operative. The last three columns headed α, β, and γ indicate the angles the cube faces, the (100) planes, make with the specimen axis.

DETERMINATION OF TENSILE PROPERTIES OF SINGLE CRYSTALS

Background

Elastic properties.- The elastic range of a solid, as defined by Hooke, is determined by the condition that the components of the stress are linearly related to the components of strain. Since aluminum is a face-centered-cubic lattice, the relations between stress and strain can be given in terms of three constants, S_{11}, S_{12}, and S_{44}. The derivation of these constants can be found in the work of Seitz (reference 5) or Zener (reference 6) and will not be repeated here. If the solid is perfectly isotropic, the constants are immediately related to the usual elastic constants, such as bulk modulus K, shear modulus G, Young's modulus E, and Poisson's ratio ν. It has been shown that

$$\frac{1}{S_{11}} = E$$

$$\frac{1}{S_{44}} = G$$

$$\frac{1}{3\left(S_{11} + 2S_{12}\right)} = K$$

$$-\frac{S_{12}}{S_{11}} = \nu$$

If the material is perfectly isotropic, it follows that

$$S_{44} = 2\left(S_{11} - S_{12}\right)$$

and the three constants are reduced to two. However, in real metals, except tungsten, this is not the case, and the ratio of the two shear constants is not equal to unity. The quantity $2\left(S_{11} - S_{12}\right)$ shall be designated as G' and the ratio of G/G' defined as the anisotropy factor A. The values of the various constants for aluminum are given below:

S_{11} (sq cm/dyne)	S_{12} (sq cm/dyne)	S_{44} (sq cm/dyne)	E (psi)	G (psi)	G' (psi)	K (psi)	ν	A
1.59×10^{-12}	-0.58×10^{-12}	3.52×10^{-12}	9.13×10^{6}	4.13×10^{6}	3.33×10^{6}	11.2×10^{6}	0.37	1.24

If aluminum were isotropic $(A = 1)$, the values of E and G would be constant, regardless of the direction. Since aluminum has an A value of 1.24, it is expected that E and G will vary with direction. The appropriate values of E and G can be computed if the direction cosines of the cubic axes with respect to the direction of stress are known. If the direction cosines are l, m, and n, the relations for the moduli are given by

$$\frac{1}{E} = S_{11} - 2\left[\left(S_{11} - S_{12}\right) - \frac{1}{2} S_{44}\right]\left(l^2m^2 + m^2n^2 + n^2l^2\right)$$

$$\frac{1}{G} = S_{44} + 4\left[\left(S_{11} - S_{12}\right) - \frac{1}{2} S_{44}\right]\left(l^2m^2 + m^2n^2 + n^2l^2\right)$$

The maximum and minimum values of E and G in units of 10^6 psi and their corresponding directions are given below:

E_{max}		E_{min}		G_{max}		G_{min}	
Value (psi)	Direction	Value (psi)	Direction	Value (psi)	Direction	Value (psi)	Direction
11.02×10^{6}	[111]	9.13×10^{6}	[100]	4.13×10^{6}	[100]	3.6×10^{6}	[111]

It is interesting to note that the application of the common equation $\nu = \frac{E}{2G} - 1$ can lead to serious discrepancies, even in a near-isotropic metal such as aluminum. This conclusion is valid not only for single-crystal work but also in any polycrystalline metal which may exhibit preferred orientation.

The influence of temperature on the crystallographic structure of aluminum has only recently been investigated. Kochanovska (reference 7) has shown that aluminum within the range of 22° to 220° C does not exhibit any anisotropy of thermal dilatation. This is fairly good evidence that aluminum retains a cubic structure within this range. This was not the case for iron, which showed a decided anisotropy of thermal-expansion constants. It is, therefore, not possible to assume that a metal which may be cubic at one temperature will remain cubic at other temperatures, even though there is no known allotropic transformation.

Critical shear strength.- The application of sufficiently large stresses to a metal will result in some permanent deformation when the stresses are removed. It has been found that when the stress exceeds a certain critical value part of the elongation has become permanent. This stress has become popularly known as the critical resolved shear stress. Although it is thought to be a constant for any one metal, the absolute value probably depends on the sensitivity of the strain measurements. The mode of deformation for aluminum is known as slip, or the displacement of one part of the crystal relative to another, along a certain crystallographic plane. Thus, when the stress exceeds a critical value on a crystallographic plane, slip occurs.

The critical resolved shear stress for aluminum is found to vary widely with investigators and purity of the metal used. Gough and Sopwith (reference 8) found the critical resolved shear stress to vary from 220 to 1600 psi. Miller and Milligan (reference 9) found the critical resolved shear stress for 99.95 percent aluminum to vary from 70 to 300 psi, with the average between 175 and 200 psi. Using constant-load-rate tests, they found a marked yield point which becomes more marked the lower the test temperature and the purer the metal. Their exploration for the yield-point behavior is based on the fact that, once the critical resolved shear stress is exceeded, the crystal may glide a considerable amount before strain-hardening becomes effective. Since this only occurs at low temperatures, they assume that the face-centered-cubic metals are softer and there is less tendency for the glide planes to rumple. The critical resolved shear stress was found to increase with temperatures up to the recrystallization range (200° to 300° C).

Boas and Schmid (reference 10), on the other hand, found no apparent yield point in aluminum single crystals in the range of -185° to 600° C. The critical resolved shear stress at -150° C was 1100 psi and decreased to 142 psi at 600° C.

Bragg (reference 11) has theoretically calculated the critical resolved shear stress in terms of atomic displacements. The method is based on the lower limiting crystallite size as determined by Wood (reference 12). This dimension was obtained by measuring the size of the crystallites produced by severe cold-work. These are assumed to be cubes, and for aluminum a side dimension of 1×10^{-4} centimeter was obtained. It should be noted that again temperature of deformation and purity of metal will affect the size of the crystallites. Bragg then assumed that the metal could withstand a shearing stress of $GS/t \approx 1000$ psi without slip occurring where

G shear modulus; 3.6×10^{6} psi

S interatomic distance; 1.12×10^{-8} inch

t size of crystallite; 3.94×10^{-5} inch

He finds that this value agrees well with measured values of 1100 psi. It is apparent that this figure is well above that observed by other investigators.

From the widely varied values of critical resolved shear stress cited above, it is evident, barring experimental errors, that a variable in addition to temperature and purity is operative. It is proposed that crystal perfection is an important, although often neglected, factor. If the crystal contains a great number of imperfections it is expected to be "softer" or exhibit nonelastic behavior sooner than a perfect crystal. An indication of the validity of this assumption has been given by Dehlinger and Gisen (reference 13). These investigators found a difference between aluminum crystals grown from the melt and those grown by strain annealing. They showed that crystals from the melt showed plastic deformation for very small shear stresses, while strain-annealed crystals showed a pronounced shear stress. The authors conclude that a true elastic range would be established if the crystals could be produced perfectly.

Plastic properties.- In most metals, once the critical resolved shear stress is reached, additional stress is necessary for the process of slip to continue and the metal is said to "work-harden." As the crystal elongates, it is found that the lattice rotates in such a manner as to decrease the angle between the slip plane and tension axis.

The resolved shear stress on the plane is then altered from its initial value, which was given by

$$\tau = \sigma \cos \phi \cos \lambda \tag{1}$$

where

ϕ angle between normal to slip plane and tension axis

λ angle between slip direction and tension axis

The variation in the shear stress is given as a function of the extension (reference 14), thus:

$$\tau = \sigma \cos \phi \left(1 - \frac{\sin^2 \lambda}{d^2}\right)^{1/2} \tag{2}$$

where $d = (1 + \epsilon) = l_1/l_0$ or the ratio of the instantaneous length to the initial length. It is readily seen that the error due to neglecting lattice rotation is negligible for strains below 0.01.

The resolved shear strain is similarly affected by lattice rotation and has been analytically described by Schmid and Boas. It should be remembered that the shear strain is not simply the extension along the slip plane, but is the relative displacement of two slip planes of unit distance from each other. The shear strain in terms of the initial orientation and the extension is given as (reference 14)

$$\gamma_P = \frac{1}{\cos \phi} \left[\left(d^2 - \sin^2 \lambda\right)^{1/2} - \cos \lambda\right] \tag{3}$$

For strains of 100×10^{-6} or less, the relation is accurately given by:

$$\gamma_P = \frac{\epsilon}{\cos \phi \cos \lambda}$$

By definition, this plastic shear strain is different from the elastic strain in the slip direction. The elastic strain is simply the extension resolved along the slip direction and is given by

$$\gamma_E = \frac{\epsilon_E}{\cos \lambda} \tag{4}$$

The ratio of the shear stress to the elastic shear strain is termed the shear modulus G and, in terms of extension and normal stress, G is given by

$$G = \frac{\sigma \cos \phi \cos^2 \lambda}{\epsilon_E} \tag{5}$$

The total shear strain is then given as the sum of equations (3) and (5), thus

$$\gamma_T = \frac{\sigma \cos \phi \cos \lambda}{G} + \frac{1}{\cos \phi} \left\{ \left[(1 + \epsilon)^2 - \sin^2 \lambda \right]^{1/2} - \cos \lambda \right\}$$

or

$$\gamma_T = \gamma_E + \gamma_P \tag{6}$$

Therefore, for small strains, the plastic shear strain may be easily calculated, if the total strain and the stress are known.

Taylor (reference 15) has found by using large strains that the shear stress-strain curve for single crystals of aluminum is a parabola. The curve is adequately described by the relation

$$\tau = .5520\gamma^{1/2} \tag{7}$$

If this relation were found to be true for the single crystals in this investigation, it would then allow the initial strain upon loading a creep specimen to be approximated. Experimentally, this quantity is virtually impossible to measure because of the high initial rate of straining. The applications of the relations presented in this section are described in the following section.

Experimental Method Used for Critical-Shear-Stress Determination

The method used for the determination of the stress-strain characteristics of the crystals was to load using dead weights. Strain measurements were taken from resistance wire strain gages which had been mounted on the specimen.

The loading frame was constructed to take loads of 175 pounds by direct loading. The top adapter which held the specimen was fixed and so constructed that the load was applied through a ball which rested on a flat bar. This assured axial alinement of the specimen. A steel cable from the center of the lower adapter connected the adapter to the pan on which the weights could be placed. The only fixed portion was the top adapter, which was fixed by the weight of the system.

Results of previous tests indicated that the stress-strain curves from single crystals of aluminum had an extremely short linear portion. Because of this, it seemed imperative that measurements be taken accurately to 1 microinch. This was accomplished by mounting SR-4 resistance wire strain gages on the specimen and reading the difference of the output signal of a dummy gage mounted on the same material and the active gage on the specimens which underwent strain. However, the SR-4 indicator can be read accurately only to 5 microinches, but by replacing the indicator dial with a precision potentiometer which could be read to 0.05 millivolt and by calibrating, it was possible to read to 0.014 microinch. The sensitivity of the measuring system made it imperative that fluctuations due to temperature difference of active and dummy gages and capacitance pickup in lead wires from the gages to the indicators be eliminated. Shielding the lead wires eliminated the pickup. Temperature was controlled by a proportioning controller which controlled the room temperature within $\pm 0.5^{\circ}$ C. The active and dummy gages and the specimen on which they were mounted were enclosed and protected from air currents. Chromel-Alumel thermocouples were connected to a two-point recorder and read the temperature of the dummy specimen and the active specimen. The temperature of the two remained within $\pm 0.25^{\circ}$ C during the test.

Test Results

The test-result portion of the study included two degrees of purity of the aluminum. A commercial 99.95-percent-purity aluminum was investigated along with the high-purity 99:99+ percent aluminum specially obtained from the Aluminum Company of America. Three curves representative of the results are shown in figures 4, 5, and 6. The point where the curves deviate from a straight line is defined as the yield stress. It is the stress required for the initiation of slip and, when resolved to the shear stress, acting on the slip plane in the slip direction, that is termed the critical resolved shear stress. The results of all the tests on the aluminum crystals are tabulated below.

Single crystal specimen	Purity (percent)	$\cos \phi \cos \lambda$	Proportional limit, P/A (psi)	Critical resolved shear stress (psi)	Experimental E (psi)	Calculated E (psi)
5	99.95	0.434	610	264	9.7×10^6	9.9×10^6
8	99.95	.458	490	225	10.45	10.4
P-3	99.99+	.482	65	31.3	10.33	10.35
P-10	99.99+	.469	62	29.0	10.2	10.2
P-16	99.99+	.462	47.5	21.9	9.0	9.25

The calculated values of Young's modulus E were determined using the following relation:

$$\frac{1}{E} = S_{11} - 2\left[\left(S_{11} - S_{12}\right) - \frac{1}{2} S_{44}\right]\left(l^2m^2 + m^2n^2 + n^2l^2\right) \qquad (8)$$

where l, m, and n are the direction cosines of the angles between the (100) planes and the specimen axis. The data indicate good agreement between the calculated and experimental values of the modulus. It is commonly thought high-purity aluminum has no elastic range; however, these data indicate that aluminum single crystals do possess some elasticity. It is pointed out, however, that as the purity increases the magnitude of the elastic portion decreases considerably.

Since the study of creep involves stresses exceeding the proportional limit, the knowledge of the amount of plastic strain upon loading is important. In order to approximate the amount of slip, the method used in the previous section, which is described by equation (6), is applied to the data. The results for the crystals P-10 and P-16 are shown graphically in figure 7.

The plastic shear strain γ_p is calculated by subtracting the elastic component from the total strain. As it is plotted on logarithmic coordinates, the fact that it follows a straight line is evidence that its equation is in the form of $\tau = B\gamma_p^n$, where B and n are constants. The slope of this line n is approximately 0.25. Since the slope can be taken as a measure of strain-hardening of the crystal, it might be expected to increase when a greater percentage of the strain is plastic. To examine this consideration, one of the crystals, P-16, was pulled in a constant-strain-rate test. The resulting shear stress-strain curve was parabolic in shape and when plotted on logarithmic coordinates produced a straight line. This is shown as the upper curve of figure 8. The slope of this line was 0.40, indicating a steeper curve. This is often interpreted as an index of the work-hardening ability and consequently it can be concluded that the combination of plastic strains as shown in figure 8 and elastic strains influences the work-hardening ability. The dotted portion of the curve in figure 8 indicates a region where no data were taken and unfortunately must include the transition zone between the two slopes.

CREEP TESTS ON SINGLE CRYSTALS

Apparatus and Test Procedure

The test pieces used were 6 inches in length with 0.75-inch thread at each end. The reduced gage section was machined to 0.505 inch in

diameter; however, after annealing and etching, the diameters at time of loading varied from 0.502 to 0.495 inch. The gage section was 2.5 inches long, but in some specimens this entire length was not wholly a single crystal. If the specimens contained a single crystal greater than 1 inch in length in the gage section, it was possible to use them.

The loading frames used to hold the specimens during tests were built to hold loads up to 500 pounds. The equipment was designed to eliminate vibrations caused by heavy equipment operating in the building. The specimen was enclosed to eliminate the possibility that any air currents would change the temperature of the specimen during testing. A front view of the equipment is shown in figure 9. The component parts of this machine were constructed in the following manner: Eyebolts were fastened to an I-beam which ran across the ceiling of the room and to these eyebolts a 3/8-inch cold-rolled steel rod was attached and threaded at one end so that a 3/4-inch triangular-shaped piece of plywood was supported from its center. At each corner of the plywood was bolted a cylinder to act as a vibration damper.

The cylinder was threaded on one end and fitted with a cap which had a hole to allow a plunger rod to work up and down through it. On this plunger, six layers of $1\frac{3}{8}$-inch-diameter "Iso-mode" rubber were placed to act as shock absorbers. The inside diameter of the cylinder was $1\frac{5}{8}$ inch. The 1/8-inch clearance between the plunger and cylinder was enough to prevent any binding between the plunger and the side walls of the cylinder. The plunger rod which extended through the cap of the cylinder was threaded so that the rod could be secured to the top plate of the case which held the specimen.

The case itself was triangular in shape, having 3/4-inch plywood for its top and bottom plates. Two sides were covered with thinner plywood and the front was a removable piece of Lucite. The top and bottom plates of the case were equilateral triangles 12 inches on a side. In the bottom, a hole was drilled large enough to allow the bottom adapter to be attached to the specimen.

The adapters which held the specimen during testing were of 1-inch diameter, machined from 75S-T6 aluminum bar stock. The top adapter was made with a 3/4-inch hole in one end to accommodate the specimen and the other end was drilled and tapped for an eyebolt. The bottom adapter was similar to the top with one end threaded to fit the specimen but was made so that a 1/16-inch aircraft cable could be slipped through. The cable was knotted, and a metal button was soldered on in a manner which allowed the cable to come out the center of the end of the lower adapter. The cable was attached to a wooden disk 10 inches in diameter which provided a platform for the weights.

The upper adapter was attached to the top plate through a hook-and-eye arrangement. Since the top adapter was not fixed but movable, and the cable which supported the load emerged from the center of the bottom adapter, axial loading was assured. A secondary precaution taken in this respect was never to screw the specimens up tight in the adapters. By forcing the ends of the specimen against the end of the threaded hole, a slight cocking could be introduced.

This manner of loading was checked using two resistance wire strain gages mounted longitudinally on the specimen 180° apart on its circumference. The strain gages, opposing one another, were connected to an SR-4 indicator. The extension of the specimen was axial when there was no movement indicated on the SR-4 indicator.

The method employed to measure the amount of creep deformation was initially resistance wire strain gages. However, after some investigation it became evident that over a period of time creep was taking place in the bonding material. In some cases, after 400 hours under load, the gage itself could be picked off quite easily.

To overcome this difficulty, a mechanical extensometer was designed using a lever-arm system. The extensometer was made up in two separate parts, hereafter referred to as the upper and lower sections. Both were made of cold-rolled steel, ground to 1/2-inch thickness, and cut to $1\frac{1}{4}$ by 2 inches. A front view of the extensometer attached to a specimen is shown in figure 10. Both upper and lower sections of the extensometer were attached to the specimen by means of Allen screws. On the upper part a pin was mounted which acted as a fulcrum for the movable lever arm. The pin was long enough and the bearing surface of the lever arm which fitted on the pin was large enough to prevent any excess play or lateral motion of the lever arm. Attached to the lever arm 0.1 inch away from the fulcrum was an adjustable connecting rod to the lower part of the extensometer. This adjustable connecting rod made it possible to adjust to a zero reading and to use either a 1- or 2-inch gage length, depending upon the length of the single crystal. An arm similar to the movable lever arm was fastened rigidly to the upper part of the extensometer and acted as a reference point from which to read. Reference marks were scratched on the ends of the arms which could be lined up with the cross hairs of the optical comparator which was used to measure the distance between the rigid arm and the movable one. The lever-arm ratio was 100 to 1. This ratio made it possible to read to 0.25×10^{-6} inch when the 2-inch gage length was used and to 0.50×10^{-6} inch when the 1-inch gage length was used. The optical comparator used had a sensitivity of 0.000050 inch.

The initial phase of the creep-testing program was at room temperature. However, room temperature varied $\pm 5^{\circ}$ C depending upon the weather. It was imperative that the temperature of the specimen remain as nearly constant as possible because of difficulties in separating that movement of the specimen due to thermal expansion and that due to creep. Also, the mechanical extensometers made of steel introduced an error for which it was difficult to compensate. The easiest method of eliminating all these difficulties would be to keep the temperature of the room constant, and by using the following method it was possible to keep the room within $\pm 0.5^{\circ}$ C. Heating elements were placed in front of a fan, both of which were connected to a proportioning controller through a relay. The proportioning controller was connected to a Chromel-Alumel thermocouple which was placed in the air at head height. A two-point Micro-max recorder, 0° to 100° C, recorded the temperature of the air. Near to the ceiling in another corner of the room, another fan was placed which circulated the air constantly. The temperature maintained in the room was 36° C. This temperature was chosen because it was above any expected outside temperature, and thus could be easily maintained. If the room was kept at a temperature below that of the outside temperature, as the latter increased during the day the room temperature also increased.

Loading was important in this work in that the load should be applied with minimum shock. The use of the cable as a support for the weights in the manner previously described allowed the weights to rotate after loading as the cable was stretched. Rotation of the weights produced shifting of the weight which, in turn, produced minor shocks on the specimen. To prevent this, the weights were anchored to stable objects which in no way increased or decreased the load but did prevent rotation of the weights.

The load was initially applied by placing the loading pan on the extended ram of a hydraulic jack and loading the needed weights upon it. The load is then applied by allowing the ram of the jack to return slowly into the jack until the specimen is supporting the load on the pan.

The creep tests were all run under constant-load conditions rather than constant stress. Preliminary tests revealed that, for the stress levels under consideration, the creep strain would not exceed 1 percent elongation in the case of the high stress level. This being true, the error due to the reduction in area would not be greater than 1 percent. In the majority of the tests the elongation would never be greater than 0.5 percent, and hence the percentage error is reduced accordingly. Thus, although these were constant-load tests, constant stress was approximated as closely as if allowance were made to decrease the load during the test.

Results of Creep Tests

The strain-time curves are shown in figures 11 to 15. This method of plotting the data as creep strains involves the knowledge of the plastic strain produced by application of the load. Since this is an extremely difficult quantity to measure, the shear stress-strain curve has been used to approximate its magnitude. The method then consists of converting the tensile load to the resolved shear stress and reading the shear strain corresponding to this stress. This shear strain is then converted to tensile strain by means of equations (4) and subtracted from the total strain as measured experimentally. The remaining strain is then the time-dependent or creep strain.

The use of this method is based on the assumption that the plastic deformation upon loading takes place by slip. This assumption, that slip is the active mechanism of deformation for extremely small strains, appears to be justified in the light of existing information.

It can be seen from the stress levels of these tests that stresses 10 times the critical resolved shear stress are necessary before appreciable creep occurs. The slope of the straight-line portion of the creep curves is often used as an index of the rapidity of the flow process. It is estimated that all of these tests have a "creep rate" of less than 0.01 percent per 100 hours. The fallaciousness of the use of the term "secondary creep rate" is strikingly shown in figures 11 to 15. Considering crystal P-33 in figure 14, if the slope of the straight-line portion of the lower curve, where seconds are used as a time measure, is determined, it is 60 times greater than the slope of the upper or "hours" curve. It cannot be concluded that, because a creep curve becomes straight, the mechanism of creep has changed. However, the opposite assumption that one mechanism of creep is operative throughout entire tests is presumptive and without sound basis. These considerations are pertinent at this time before a detailed analysis is entered into, since they indicate the impartial character of the analysis.

The creep curves appear to be normal in shape and little can be deduced without a more detailed analysis, which will be presented in the following sections. In general, the creep strain, after the instantaneous extension has been subtracted, appears to increase more uniformly with the resolved shear stress than with the applied tensile stress. This would tend to indicate that the mechanism (or mechanisms) active in the initial deformation remains active during the creep process. It would appear from the shapes of the curves that, although this mechanism is extremely potent in its ability to allow the crystal to strain, its potency wears off very rapidly and as a result the strain rate decreases many orders in magnitude. It is at this time that if a second mechanism of creep is possible its effect becomes

important and the character of the creep curve changes. It is emphasized that these creep studies were conducted on specimens which contained no grain boundaries and therefore the usual concept of grain-boundary viscosity cannot be considered as a factor in the creep process. These creep tests are relatively short-time tests and although no indications of a third stage of creep were noticed its possibility has not been eliminated.

ANALYSIS OF CREEP TEST RESULTS USING EXISTING THEORIES

Background

At present, most of the theoretical work on creep is based on attempts to relate creep phenomena to the concept of "dislocations." In order to present the relation between the results of this investigation and current theoretical analysis, it is desirable to review briefly some of the concepts involved.

The existence of dislocations or some type of imperfection has been established on the basis of the criterion that if a crystal were perfect, that is, every atom alined with every other atom, the stress necessary to initiate slip would be 100 to 1000 times greater than has been observed experimentally. The greater theoretical strength of a regular array of atoms is due to the fact that shear can take place only by a movement of a whole plane of atoms relative to an adjoining plane.

If some simple lattice of a perfect crystal is considered, as in figure 16, simple slip requires that a certain shear stress τ cause homogeneous and reversible deformation until the shear strain is $\lambda/2d$. Beyond this point the deformation is permanent, since the displaced planes find it easier to stop at the new equilibrium position, displaced λ distance from their original positions, than return to the original position. If the shear stress τ which would cause permanent deformation were maintained for a time, the specimen would flow plasticly. The fact that this is not observed in metals indicates that some hardening is taking place as a result of the flow process.

In figure 16 plane B is in stable equilibrium with plane A before and after set B was displaced an atomic spacing λ in the slip direction. In both cases, the resultant shear stress on plane A is zero. However, for a displacement halfway between the two positions, the resultant shear stress is again zero, but set B is in an unstable-equilibrium position. This indicates that the stress on set A is periodic in X and of period λ. It is then possible to approximate the stress by a sine wave in X, such as:

$$\tau = \tau_c \sin \frac{2\pi X}{\lambda} \tag{9}$$

where τ_c is the amplitude of the stress and is large enough to bring the displacement to the halfway mark. The stress τ_c is then the largest shear stress which the lattice can withstand. Simple slip will occur for all shear stresses larger than τ_c.

The shear modulus G is related to the initial slope of the shear stress-strain curve. One can assume that the slope of the stress-strain curve of equation (9) at $X = 0$ is the same as the initial slope of the shear stress-strain curve for a specimen. For very small displacement of set A about an equilibrium position, Hooke's law might be used to calculate the stress on set A. The shear strain of set A with respect to set B would be X/d. Then, from Hooke's law, the stress τ is found to be equal to GX/d, where G is the modulus of rigidity. By substituting into equation (9), the following relation is evolved

$$\frac{2\pi}{\lambda} \tau_c = \frac{G}{d}$$

and, since λ/d is nearly equal to 1,

$$\tau_c = \frac{G}{2\pi} \tag{10}$$

Of course such a relation does not hold experimentally, but it does provide a starting point for further calculation of the strength of metal crystals.

It would be best before progressing any further in this direction to describe the different types of dislocations. The simplest type, the edge dislocation, is shown by figure 17. A dislocation as pictured arises over a limited distance in a plane of atoms where there are n atoms in one plane and $n + 1$ in the adjoining plane. In figure 17(a), the compressed region, where the plane with the excess atom is above the expanded plane with one less atom, the dislocation is called a positive dislocation. In figure 17(b), where the reverse is true, the dislocation is a negative one. This concept of dislocations was first described by Taylor (reference 16).

The second fundamental type of dislocation is the screw dislocation introduced by Burgers (reference 17). The structure of a screw dislocation is shown in figure 18. Slip is produced by migration of the dislocation region EF toward CD. In the diagram the full lines and circles represent the atoms of the upper plane, while the others are the lower plane. It is possible to have positive and negative

screw dislocations where, as in edge dislocations, one is the reverse of the other.

Since the strength of crystalline material is lower than the predicted theoretical strength, it can be assumed that dislocations are inherent to crystalline materials. The origin of these dislocations is still not certain, but it is thought that they originate from points of imperfections in the lattice of the crystal. In polycrystalline material the grain boundaries present places of irregular array of atoms, a sort of a transition layer between grains, and thus may constitute a source of dislocation. However, the present work does not include grain boundaries. The existence of a mosaic structure within the grain has been postulated by Darwin (reference 4) as a result of his study of the intensity of X-ray diffraction spots in metals. He concluded that crystals diffract as if they were composed of small blocks 10^{-4} to 10^{-6} centimeter on an edge, but each block being a perfect crystal tilted from perfect alinement by 0.1°.

Wood (reference 12), using various high-purity metals, determined the lower limit of crystallite size to be as follows:

Metal	Purity (percent)	Crystallite size (cm)
Copper	99.999	8.7×10^{-5}
Nickel	99.97	1.2
Silver	99.999	.8
Iron	99.96	3.2
Aluminum	99.99	10.0

Barrett (reference 18) was able, using electron-microscope technique, to make photomicrographs of deeply etched copper in which he showed what he assumed to be mosaic imperfections in the crystal. The mosaics were rod-shaped, equiaxed in cross section, and had diameters 1×10^{-5} to 5×10^{-5} centimeter and lengths up to 5×10^{-4} centimeter.

The establishment of the fact that a crystal is composed of many small blocks whose orientations vary slightly with respect to one another presents places at which dislocations may exist. The majority of dislocations probably exist here, but there are other places such as inclusions and precipitated atoms that also could be sites for dislocations. The number of dislocations that could form between disoriented blocks would, it seems, be determined by the degree of disorientations; that is, the density of the dislocations increases with an increase of the angle between blocks. Burgers' work (reference 19)

shows that lattice blocks, which are nearly parallel, can be separated by systems of dislocations. Here these systems must contain an equal number of dislocations of both signs and exist as a result of cold-work, and hence are energetically unstable. The nature of a dislocation is such that each is surrounded by a region of localized strain, thus subjecting atoms in this region to internal stresses. These regions exert forces on each other which, in the case of a positive and negative dislocation, attract one another, while dislocations of like signs repel each other.

The initial movement of a dislocation is dependent upon the temperature and the stress. The activation energy of a dislocation, the energy required to move it, is dependent upon its position in the atomic lattice plane. Due to the interaction of the atoms and the negative and positive dislocations, the potential energy will be an oscillatory function of distance along the plane under consideration, as in figure 19.

A dislocation at rest would be in some potential trough such as A and in order to move to position B would have to receive the amount of energy ϕ, the activation energy. The fact that the amount of energy could be produced by thermal fluctuations is a finite probability. This probability will vary with the absolute temperature T and the activation energy ϕ according to $e^{-(\phi/kT)}$, where k is Boltzmann's constant. Since this probability is an exponential, as the temperature becomes high there is a real probability of movement of dislocations such that they can overcome large potential barriers.

The stress tends to change the potential-energy function, depending upon the magnitude of the stress. This has the effect, as shown by the dotted line in figure 19, of reducing the barrier in one direction and increasing it in the opposite direction.

This extremely brief review of the dislocation theory is meant only as an introduction to the thinking which underlies present-day theory. Much of the mathematics and detailed derivations have been eliminated. The reader is referred to such excellent articles as references 5, 20, 21, and 22 for further information.

Creep Theories

Among the contributors to the theories of transient creep are Mott and Nabarro (reference 22), Smith (reference 21), Orowan (reference 20), and Andrade (reference 23). Really, the last named was the first to evolve a practical relation. However, as discussed in the body of this report, his relation does not appear to be applicable to these data and hence will not be considered here. Orowan has a

particularly neat theory, but again his theory has the same failing as Andrade's. A complete description of Orowan's theory is given in reference 24. The field is then narrowed down to two theories, that of Mott and Nabarro and that of Smith.

The first to be discussed here is that of Mott and Nabarro. The basis of this development is that dislocations of a compound type are assumed. Whenever this dislocation intercepts a glide plane, a wavy line is formed. Normally, dislocations tend to take up positions of minimum potential energy; however, because of the curvature, the dislocation possesses a higher energy. The condition is assumed that each dislocation has a different value of internal stress to overcome before it can move.

With this picture, an expression for creep was formulated using the following assumptions:

(1) A distribution function $N(\sigma_i)$ was defined such that $N(\sigma_i)d\sigma_i$ gives the density of the dislocation loops which would be moved at a stress between σ_i and $\sigma_i + d\sigma_i$.

(2) The distribution function $N(\sigma_i)$ does not change appreciably during creep, hardening being primarily due to the exhaustions of dislocations.

(3) A dislocation loop tends to move from a position where the stress increment required to move the dislocation loop is small to a position where the stress needed to move it is much larger than the applied stress. Once the loop moves, it does not again take part in the creep.

(4) The probability P that a dislocation loop with a given value of σ_i will move in the direction of the applied stress is an exponential involving the absolute temperature T,

$$P = \nu \exp(-Q\sigma_i/kT)$$

where $Q(\sigma_i)$ is the activation energy for migration and ν is the frequency of vibration of a dislocation in its potential trough (10^8 vibrations per sec).

This results in an increase of strain equal to ν divided by the volume of the crystal. The value of ν depends on whether or not the motion of a single loop sets off an avalanche and cannot be evaluated at this time.

After a time t, the number of remaining dislocations in the range σ_i to $\sigma_i + d\sigma_i$ which have not moved is $N(\sigma_i)d\sigma_i e^{-Pt}$ and their contribution to the creep rate is obtained by multiplying by Pv. The creep rate is then:

$$\frac{d\epsilon}{dt} = Pv \int_{\sigma}^{\infty} N(\sigma_i) e^{-Pt} \, d\sigma_i$$

Evaluating this integral, Mott and Nabarro find that the extension is given in terms of t by the formula of the type:

$$\epsilon = \text{Constant } T^{2/3} \left(\log_e \nu t\right)^{2/3} \tag{11}$$

Smith (reference 21) has developed a theory of transient creep which avoids the difficulty of Orowan's assumption that each activation is accompanied by glide inversely proportional to ΔT^2. His theory is based on the assumption that after the initial almost instantaneous elongation there will be regions in the material where there are stress concentrations, so that the local stress is higher than the mean applied stress. These could be caused by points of entrapped dislocations, for example, at mosaic boundaries or at impurities. Due to the stress concentrations at various energy levels E and $E\,dE$, there will be a relationship between the number of such spots $f(E)\,dE$ and the distribution function $f(E)$ which changes as plastic flow progresses. By assuming that the distribution function $f(E)$ changes with time and denoting this function by F, he proceeds to calculate the number of spots lost during a time dt. He assumes that these spots are lost by thermal activation, and that this number dN is given by

$$dN = C(F_o \, dE)e^{-(E/kT)} \, dt$$

Smith then shows this equation has a solution of the form

$$F = F_o e^{-\lambda t}$$

where $\lambda = Ce^{E/kT}$ and F_o is the initial condition at $t = 0$. By various manipulations, he arrives at the expression for the creep rate

$$\frac{d\epsilon}{dt} = aF_o kT\left(\frac{1 - e^{-Ct}}{t}\right)$$

where a is the amount of glide from a single activation.

The creep rate is then proportional to the function $F(t)$ and the absolute temperature, and $F(t)$ is defined as:

$$F(t) = \frac{1 - e^{-Ct}}{t}$$

If $Ct \ll 1$, $F(t)$ is a constant since the expansion e^{-Ct} involves higher powers of Ct and $\epsilon = \int_0^t \frac{d\epsilon}{dt} = aF_0kT(Ct)$. But if $Ct \gg 1$, $F(t)$ approximates $1/t$ and

$$\epsilon = \text{Constant } (aF_0kT) \log_e (\text{Constant } t) \tag{12}$$

Since C is of the order of Mott and Nabarro's ν, 10^8 to 10^{10} vibrations per second, the assumption that $C \gg 1$ is justified and the creep depends logarithmically upon time, as in equation (12).

Analysis of Creep Results on Basis of Movement of Dislocations

The shapes of the creep curves for aluminum single crystals are peculiar in that the extremely rapid strain rate dies out quickly, more quickly than has been observed in previous experiments. The suggestion that the ability of a crystal to strain can be exhausted leads to the examination of the theory of Mott and Nabarro (reference 22). Their analysis of the mechanism of creep is based on dislocations and the ability of these dislocations to move and propagate in a metal. Their theory recognizes that transient creep is a manifestation of two distinct mechanisms which may or may not take place simultaneously. The first mechanism postulates that the dislocation loops move in a metal but do not generate new dislocations. Eventually straining will cease because of the exhaustion of energetically favorable dislocations. This type of creep occurs at low stresses and low temperatures and in hardened metals. The second type of transient creep is associated with multiplication of dislocations. This type of creep is the more common of the two and is probably the type used in the evaluation of the $t^{1/3}$ relation.

It is the first type of creep, or the exhaustion creep, that the experimental data seem to follow. A characteristic of this type of creep is that the instantaneous extension is much greater than the time-dependent extension. Exhaustion creep is expected to follow the relation:

$$\epsilon = CT^{2/3} (\log_e \nu t)^{2/3} \tag{11}$$

where

ϵ creep strain

T absolute temperature, ^{o}K

ν frequency of vibration of a dislocation; approximately 10^{8} vibrations per second

t time, seconds

C constant which varies directly with applied shear stress

Relation (12), developed by Smith in reference 21, also applies to transient creep:

$$\epsilon = \text{Constant } T \log_e(\text{Constant } t) \tag{12a}$$

It is evident that this equation is analogous to that of Mott and Nabarro and differs only in the exponents of temperature and time. In Smith's relation, the exponent is unity; in Mott and Nabarro's, it is 2/3.

The results of attempts to fit the two theories to the initial portion of the creep curves are shown in figures 20 to 24. The method of fitting the relations to the experimental data was similar to that used for Andrade's relation. The experimental and theoretical relations were assumed to coincide at one of the early strains. From this point, the rest of the theoretical curve was determined. Although Smith's relation is plotted for only one of the curves it was tried for all, and the agreement was poor. On the other hand, Mott and Nabarro's relation provided a good fit with the experimental data in all but one case (crystal P-41). This crystal was subjected to the highest stress and is probably outside the boundaries of exhaustion creep. It was further noted that this crystal was the most favorably oriented for slip ($\cos \phi \cos \lambda = 0.5$) and presented a second favorable system for slip which enhanced the possibilities of duplex slip and, consequently, higher orders of strain were possible.

It can be concluded that the application of the concept of dislocations to transient creep results in an analysis that agrees favorably with experimental data. It would be interesting to evaluate the constant in Mott and Nabarro's relation; however, further analysis would be based on uncertain assumptions and is not warranted at this time.

From this analysis, a general picture of the process of creep in aluminum single crystals at relatively low temperatures can be drawn. When a load is applied to a crystal the dislocations which are present

propagate and grow. It would appear that the criterion for their growth is their orientation with respect to the applied stress. When the stress is maintained constant, a time-dependent strain becomes evident. This is a manifestation of the statistical distribution of the dislocations. In other words, the probability that there will be dislocations for which the energetics will be favorable for movement decreases exponentially with time. Therefore, the rate of straining will decrease with time, asymptotically approaching zero. The fact that this has not been observed in these tests can be attributed to one of two reasons: (1) The tests were stopped before reaching their limiting creep strain, or (2) another mechanism became operative after the available dislocations were used up.

The latter of the two reasons is the more thought producing. If the dislocations have moved, the cessation of movement is due either to their removal from the crystal or a mutual blocking effect. If the dislocations are blocked or trapped, it is reasonable to assume that their mutual free energy is a minimum and that they form some sort of a stable array. The additional strain is then the result of the movement of the small semiperfect lattice blocks, bounded by these arrays of dislocations, relative to one another. This could conceivably lead to a viscous type of creep in a single crystal.

Correlation of Creep Results with Work of Andrade

While the expression for creep developed by Andrade (reference 23) nearly 40 years ago has no basic theoretical foundation, such as the concept of dislocations, it has frequently been used to describe creep phenomena. Accordingly, the data obtained here were used in connection with Andrade's expressions.

In his original study, polycrystalline wires of various metals were used and the tests carried out under constant-stress conditions. Since then, his relation has been confirmed for aluminum and zinc single crystals. In the tests on aluminum single crystals reported by Orowan (reference 20) it must be pointed out that the stresses were considerably higher (10 times) than in the tests described in this report. Since Orowan's tests lasted only 30 minutes, and the strain exceeded 3 percent, there is some doubt as to the validity of his interpretation of the phenomenon as a true creep process.

Andrade, in his analysis, divides creep into two stages: Transient and quasi-viscous. His empirical relation is

$$l = l_o\left(1 + \beta t^{1/3}\right)e^{kt} \qquad (13)$$

where

l length of specimen at any time t

l_o length associated with initial extension obtained upon loading

β, k constants

Now, if l_o' is the unstretched length or the length at the time $t = 0$, then the strain ϵ_o associated with l_o will be $\epsilon_o = \left(l_o - l_o'\right)/l_o'$, so $l_o = l_o'\left(1 + \epsilon_o\right)$.

Substituting into equation (13),

$$l = l_o'\left(1 + \epsilon_o\right)\left(1 + \beta t^{1/3}\right)e^{kt} \tag{14}$$

For relatively short times the effect of the e^{kt} is small and the term may be neglected. Then

$$l = l_o'\left(1 + \epsilon_o\right)\left(1 + \beta t^{1/3}\right)$$

Neglecting that part of the product which is very small, $\epsilon_o \beta t^{1/3}$, then

$$l = l_o'\left(1 + \epsilon_o + \beta t^{1/3}\right) \tag{15}$$

The total strain at any time t will be $\epsilon = \dfrac{l - l_o'}{l_o'}$. Equation (15) then becomes

$$\epsilon = \epsilon_o + \beta t^{1/3} \tag{16}$$

where ϵ is the total strain, ϵ_o is the strain associated with l_o, and β and t are the same as in equation (13).

The term l_o in the Andrade relation has a certain physical significance attached to it by Andrade (references 23 and 25) and Orowan (reference 20). It is the length that is larger than the unstretched length l_o' and is associated with that extension accompanying the application of the load. However, it is essentially a third empirical constant of the relation. It cannot be determined experimentally because it is difficult to determine when the extension due to the application of the load ceases and creep begins.

From the data obtained in this investigation it was possible to determine analytically the value of ϵ_o associated with the length l_o. For times greater than 400 seconds ϵ and t were obtained experimentally. By substituting these values of ϵ at various times t, a simultaneous equation was set up to evaluate β and ϵ_o.

The value of ϵ_o obtained in this manner did not agree with that obtained by the method described earlier in the report. That determined by Andrade's method was larger by nearly a factor of 2 at all stress levels investigated.

In most of the data to which Andrade's relation has been applied it is found that the strains are usually greater than 0.1. In the tests described in this report the creep strains are less than 0.005, or 20 times smaller than the previously mentioned creep strains. If Andrade's relation can be shown to describe these data, then further support has been found for its acceptance in the range of strains usually associated with creep. However, efforts to achieve any fit were not successful. In all cases Andrade's relation predicted larger creep strains than were observed experimentally.

The method of examining the data was to plot the creep strain (initial extensions had been subtracted) on logarithmic coordinates. If Andrade's relation holds, a straight line should result with a slope of 0.33. It is proper to expect a straight line only in the very first portion of the creep test, for as the test progresses the creep strain should be greater than that predicted by the $\beta t^{1/3}$ term. Hoever, in analyzing these data, it was found that the experimental creep strains were not so large as predicted theoretically. A further point of interest was that the slope of the straight-line portion was smaller than 0.33. It ranged from 0.02 for crystal P-37 to 0.20 for crystal P-33. It appeared to increase with stress, the one exception being P-41, which had a slope of 0.08.

The variation of the exponent from 0.33 had been found previously by Smith (reference 6), who reported a value of 0.1 provided a good fit for a room-temperature creep test on polycrystalline copper. An example of the grossness of the discrepancy between the experimental and theoretical curves is shown in figure 25. It is strikingly indicated how the experimental curve falls off very rapidly. It is also evident there can be no quasi-viscous component based on this analysis, since k would have to be negative and no physical significance can thus be attached to this value.

From the results of this comparison it would appear that the crystal crept very rapidly for an extremely short period of time and then, for some reason, its ability to creep was lost, or its resistance to further movement increased. A possible argument as to the lack

of agreement might stem from the fact that these were constant-load, not constant-stress, tests. If this were a factor, the creep strain would be expected to be greater, not smaller, than predicted from theory.

CONCLUSIONS

The most important conclusions from this study of creep of aluminum single crystals are:

1. High-purity (99.99+-percent-aluminum) crystals grown by the strain-anneal process possess a definite elastic range. The critical resolved shear stress is between 20 and 30 psi.

2. This critical shear stress must be greatly exceeded (10 times) before appreciable creep will take place.

3. The amount of creep appears to be more directly related to the resolved shear stress than to the tensile stress.

4. The shape of the curves indicates an exhaustion type of creep as originally proposed by Mott and Nabarro. The data also serve as one of the first proofs as to the validity of their relation.

5. Creep can be adequately qualitatively described in terms of the dislocation theory. Additional tests at various temperatures and stresses are necessary for a quantitative evaluation of the constants present in the analytical relations.

Battelle Memorial Institute
Columbus, Ohio, September 26, 1950

REFERENCES

1. Carpenter, H. C. H., and Elam, C. F.: Experiments on Distortion of Single Crystal Test Pieces of Aluminum. Proc. Roy. Soc. (London), ser. A, vol. 107, no. 742, Feb. 2, 1925, pp. 171-180.

2. Smith, D. W.: Discussion of: "Recrystallization of Aluminum and Aluminum Alloys" by L. W. Eastwood, R. W. Jones, and R. F. Bell. Trans. Am. Inst. Min. and Met. Eng., vol. 133, 1939, pp. 139-140.

3. Burke, J.: The Fundamentals of Recrystallization and Grain Growth. Grain Control in Industrial Met., Am. Soc. Metals Educational Ser., 1949.

4. Barrett, C. S.: Structure of Metals. McGraw-Hill Book Co., Inc., 1943.

5. Seitz, F.: The Physics of Metals. McGraw-Hill Book Co., Inc., 1943.

6. Zener, C.: Elasticity and Anelasticity of Metals. Univ. of Chicago Press, 1948.

7. Kochanovska, A.: Investigation of Thermal Dilatation of Cubic Metals. Physica, vol. 15, Noe-2, April 1949, pp. 191-196.

8. Gough, H. J., and Sopwith, D. G.: Behavior of a Single Crystal of Aluminum under Alternating Torsional Stresses While Immersed in a Slow Stream of Tap Water. Proc. Roy. Soc. (London), ser. A, vol. 135, no. 826, Feb. 1, 1932, pp. 392-411.

9. Miller, R. F., and Milligan, W. E.: Influence of Temperature on Elastic Limit of Single Crystals of Aluminum, Silver, and Zinc. Trans. Am. Inst. Min. and Met. Eng., vol. 124, 1937, pp. 229-245.

10. Boas, W., and Schmid, E.: Neber die Temperaturabhaengigkeit der Kristallplaztizitaet. III Aluminum. Zeitschr. Phys., Bd. 71, 1931, pp. 703-714.

11. Bragg, W. L.: A Theory of the Strength of Metals (Crystallites). Nature, vol. 149, no. 3784, May 9, 1942, pp. 511-513.

12. Wood, W. A.: The Lower Limiting Crystallite Structure Size and Internal Strains in Some Cold-Worked Metals. Proc. Roy. Soc. (London), ser. A, vol. 172, no. 949, Aug. 3, 1939, pp. 231-241.

13. Dehlinger, U., and Gisen, F.: Plastizitat und Mosaikstruktur bei gegossenen und bei rekristallisterten Metallen. Zeitschr. Phys., Bd. 35, 1934, pp. 862-864.

14. Schmid, E., and Boas, W.: Plasticity of Crystals. F. A. Hughes and Co., Ltd. (London), 1950.

15. Taylor, G. I.: The Distortion of Crystals of Aluminum under Compression. Parts II and III. Proc. Roy. Soc. (London), ser. A, vol. 116, no. 773, Sept. 1, 1927, pp. 16-60.

16. Taylor, G. I.: The Mechanism of Plastic Deformation of Crystals. Proc. Roy. Soc. (London), ser. A, vol. 145, no. 855, July 2, 1934, pp. 362-404.

17. Burgers, J. M.: Geometrical Considerations Concerning the Structural Irregularities to be Assumed in a Crystal. Proc. Phys. Soc. (London), vol. 52, no. 1, Jan. 1, 1940, pp. 22-33.

18. Barrett, C. S.: Metallography with Electron Microscope. Trans. Am. Inst. Min. and Met. Eng., vol. 156, 1944, pp. 62-80.

19. Burgers, W. G.: Recovery and Recrystallization Viewed as Processes of Dissolution and Movement of Dislocations. Proc. Roy. Soc. Amsterdam, vol. 50, nos. 1 to 5, March to April 1947, pp. 452, 495, 719, and 858.

20. Orowan, E.: The Creep of Metals. Jour. West of Scotland Iron and Steel Inst., vol. 54, 1946-1947, pp. 45-82.

21. Smith, C. L.: A Theory of Transient Creep in Metals. Proc. Phys. Soc. (London), vol. 61, no. 3, Sept. 1, 1948, pp. 201-205.

22. Mott, N. F., and Nabarro, F. R. N.: Dislocation Theory and Transient Creep. Rep. Conf. on Strength of Solids, Phys. Soc., 1948, pp. 1-19.

23. Andrade, E. N. daC.: On the Viscous Flow of Metals and Allied Phenomena. Proc. Roy. Soc. (London), ser. A, vol. 84, no. 567, June 9, 1911, pp. 1-12.

24. Schwope, A. D., and Jackson, L. R.: A Survey of Creep in Metals. NACA TN 2516.

25. Andrade, E. N. daC.: The Flow of Metals under a Large Constant Stress. Proc. Roy. Soc. (London), ser. A, vol. 90, no. 619, July 1, 1914, pp. 329-342.

TABLE 1.- CRYSTALLOGRAPHIC DATA FOR SINGLE CRYSTALS USED IN TESTS

Specimen	Slip plane	ϕ (deg)	Slip direction	λ (deg)	cos ϕ cos λ	α (deg)	β (deg)	γ (deg)
P-3	D	44	V_{DC}	51	0.482	48	38	8
	A	27	Y_{AB}	64	.391			
	D	44	Z_{AD}	58	.387			
	B	89	W_{CB}	70	.305			
P-10	B	56	U_{BC}	33	0.469	22	63	17
	A	61	Z_{AC}	28	.428			
	D	27	Y_{AD}	65	.377			
	D	27	V_{BD}	68	.334			
P-13	A	54½	Z_{AD}	36	0.470	22½	62½	15
	B	64	U_{BD}	26	.394			
	C	28	V_{BC}	76	.387			
	C	28	X_{AC}	10	.317			
P-16	B	50½	U_{BC}	43½	0.462	8	81½	2
	D	47½	Y_{AD}	47	.457			
	D	47½	U_{BD}	53	.407			
	A	59	Z_{AC}	37	.405			
P-22	C	58	Z_{AB}	35½	0.431	29½	54	20½
	D	68½	X_{AD}	25	.332			
	C	58	W_{CD}	53	.319			
	B	18½	U_{BD}	72	.293			
P-33	B	49½	Z_{AB}	45	0.459	14	49	37½
	B	49½	U_{BC}	53	.391			
	D	22	W_{CD}	69	.332			
P-37	D	60	X_{AD}	31	0.429	22	67½	32½
	C	61½	Z_{AC}	29½	.415			
	B	22	U_{BC}	70½	.310			
P-40	A	45½	Z_{AD}	46	0.487	8½	31	57½
	C	36	U_{BC}	60½	.429			
	A	45½	X_{AB}	62	.329			
P-41	D	46	W_{CD}	44	0.500	66	23½	6
	A	36	Z_{AB}	55	.464			
	B	68½	V_{BC}	22½	.339			

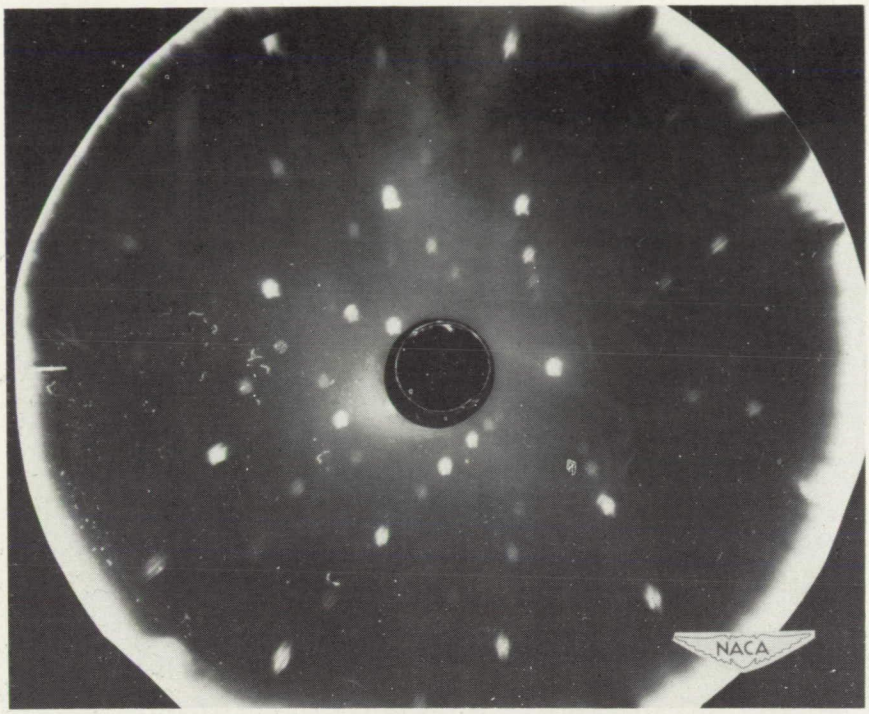

Figure 1.- Lauegram of a single crystal of aluminum. Location 1.

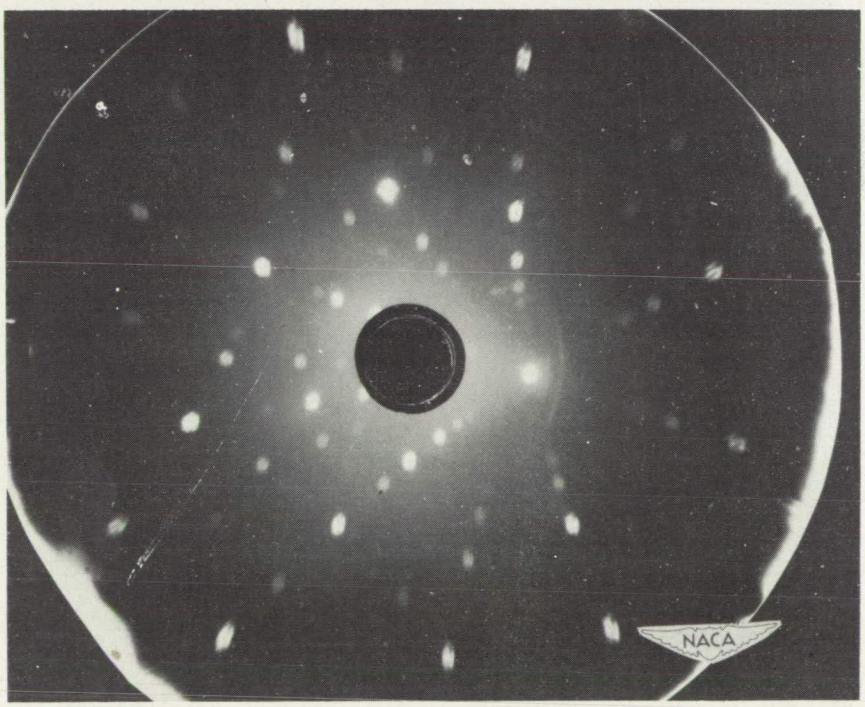

Figure 2.- Lauegram of a single crystal of aluminum. Location 2.

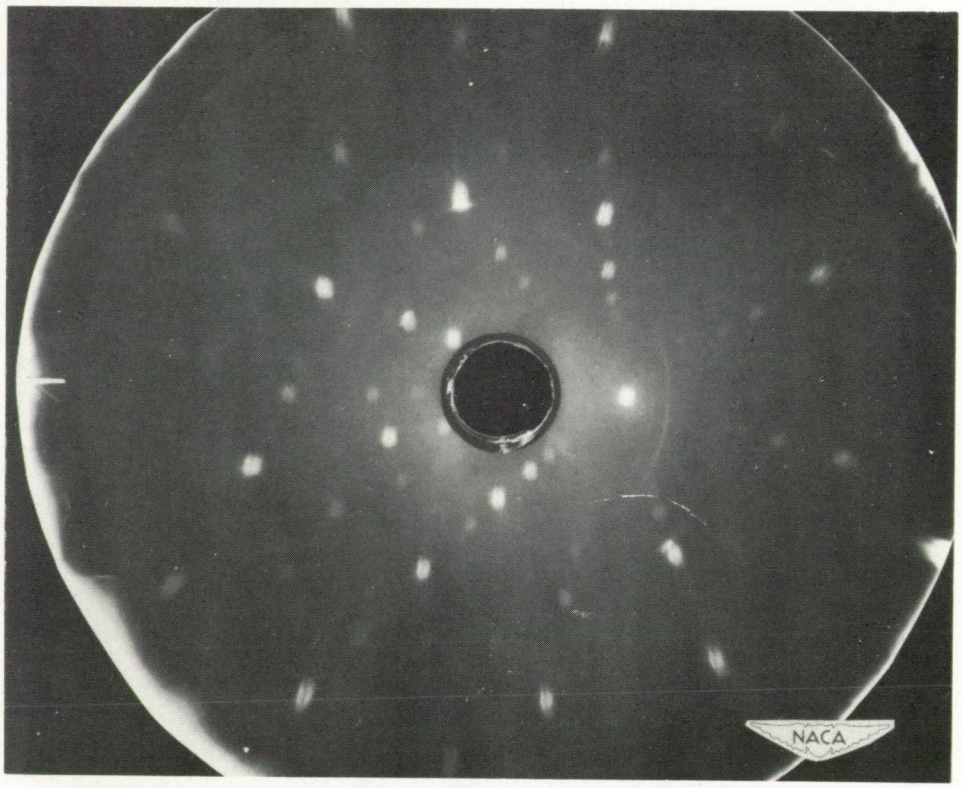

Figure 3.- Lauegram of a single crystal of aluminum. Location 3.

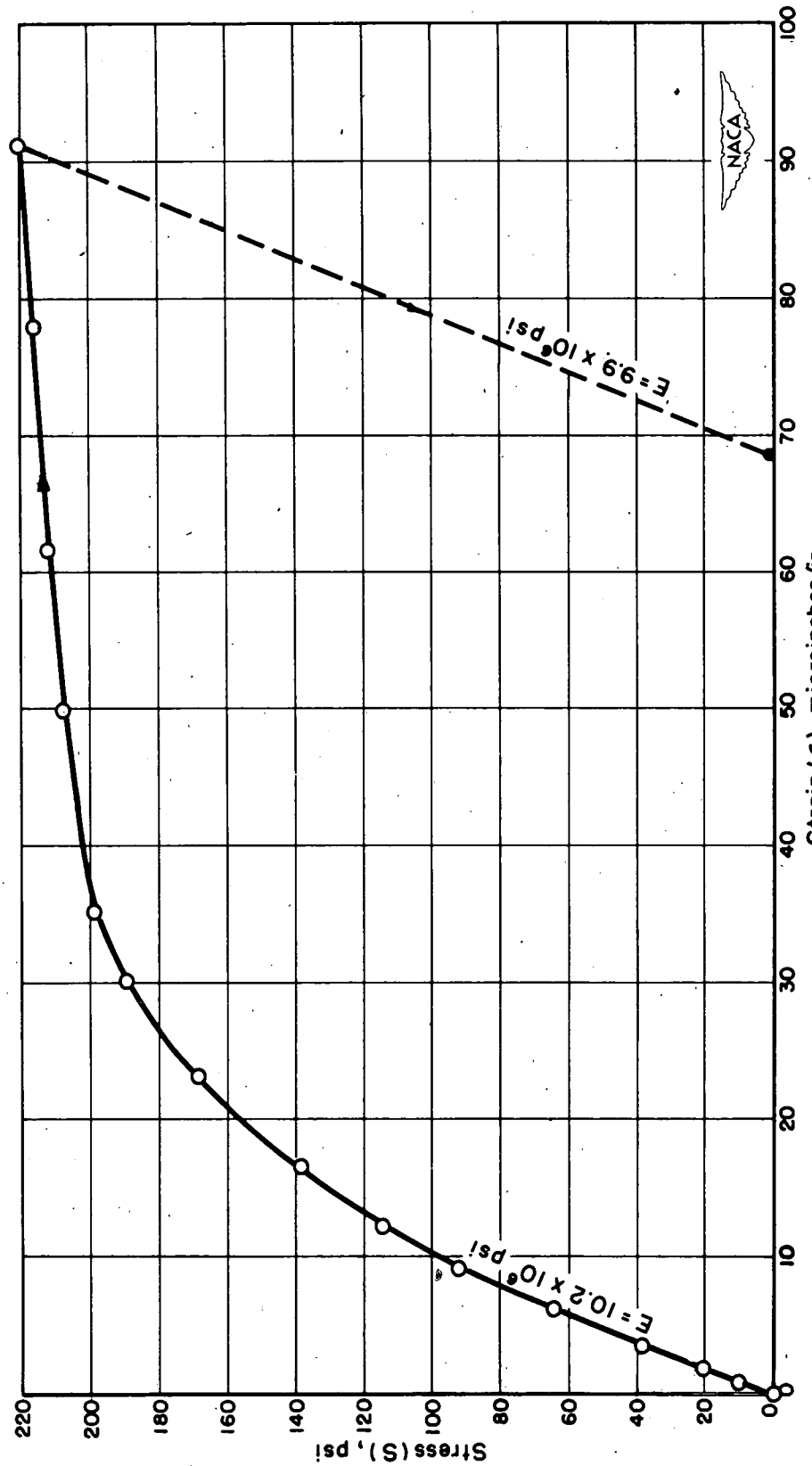

Figure 4.- Tensile stress-strain curve for a single crystal of aluminum (99.99+ percent pure). Crystal P-10.

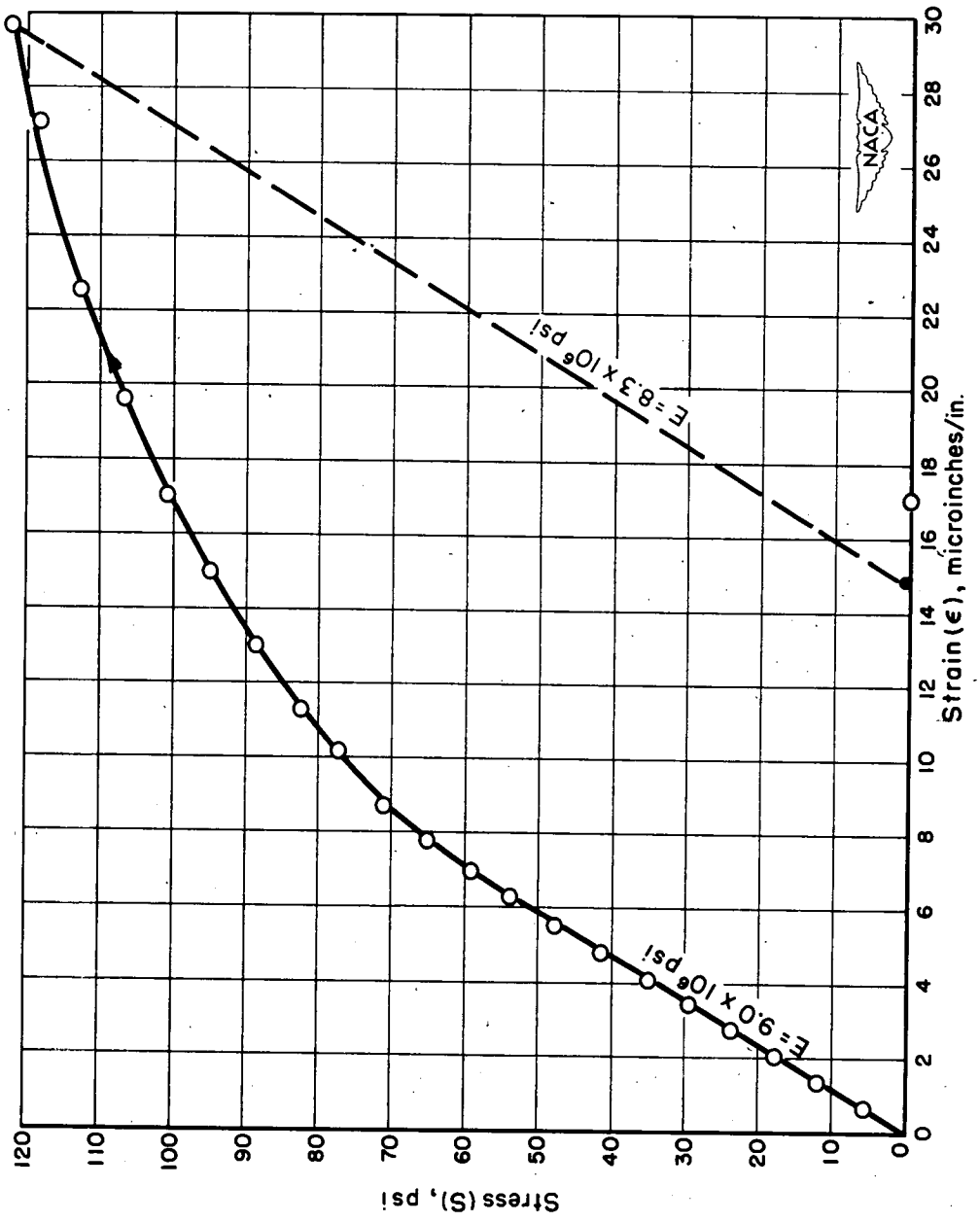

Figure 5.- Tensile stress-strain curve for a single crystal of aluminum (99.99+ percent pure). Crystal P-16.

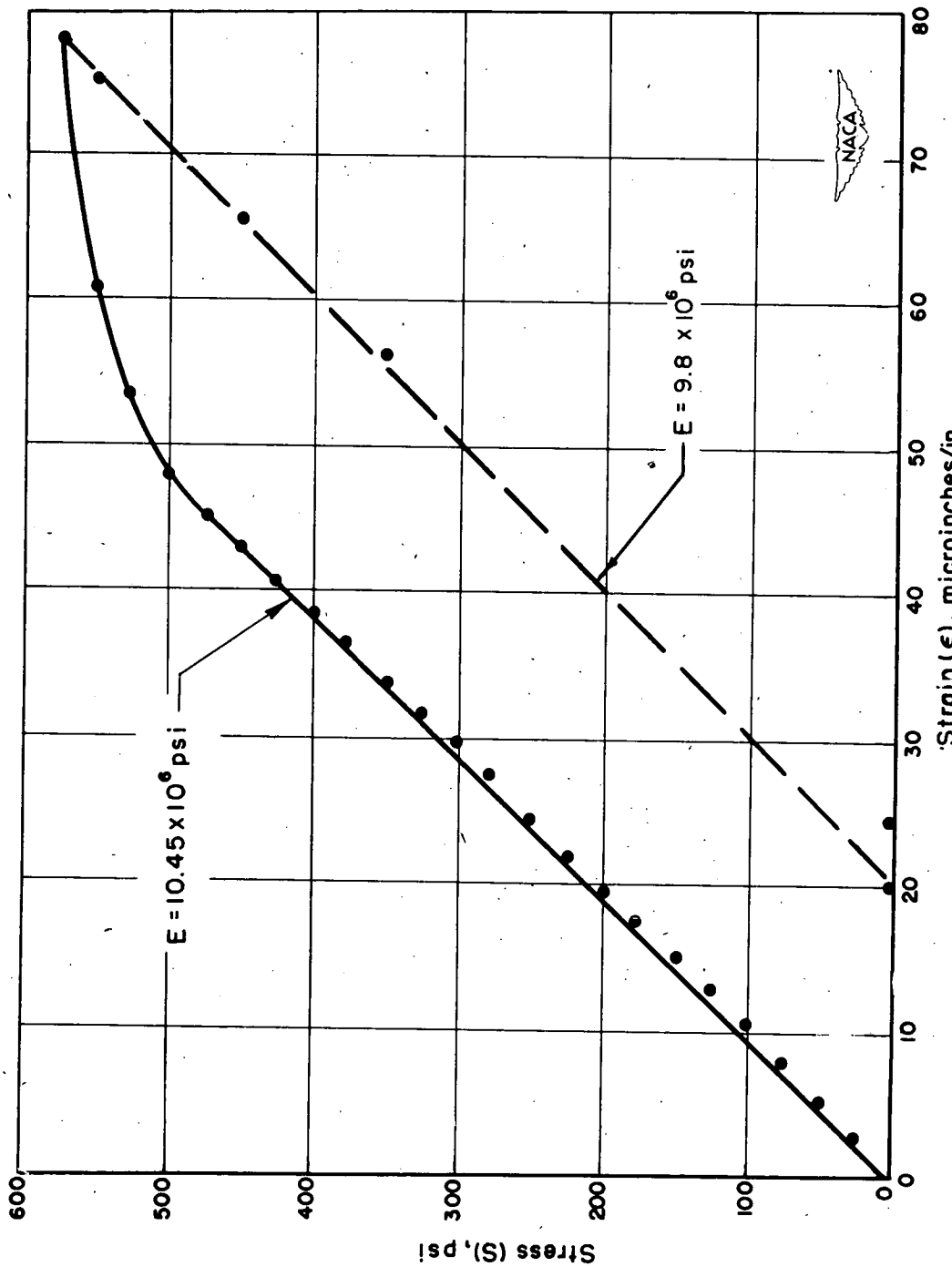

Figure 6.- Tensile stress-strain curve for a single crystal of aluminum (99.95 percent pure). Crystal 8.

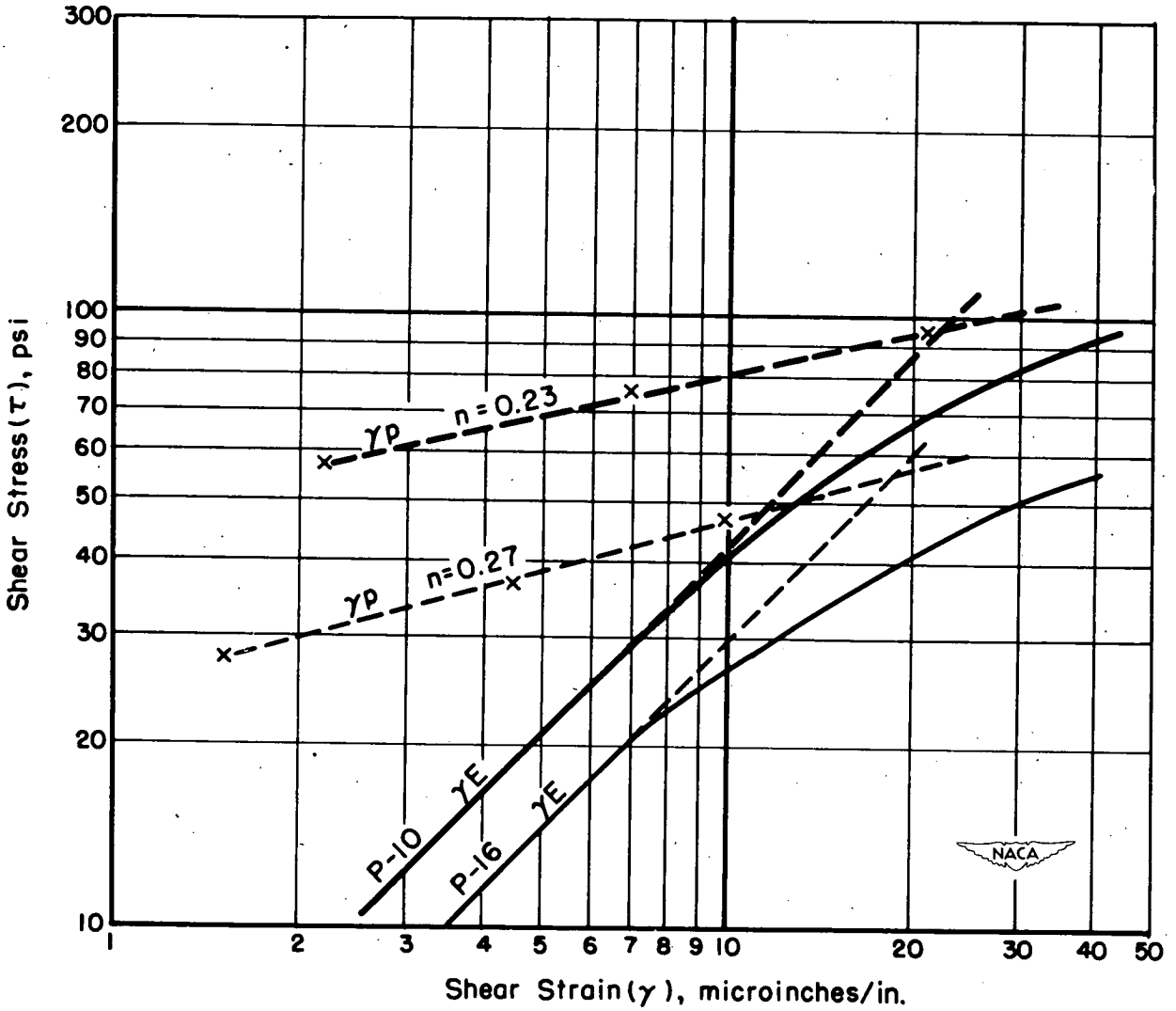

Figure 7.- Resolved shear stress-strain curves for single crystals of aluminum (99.99+ percent pure).

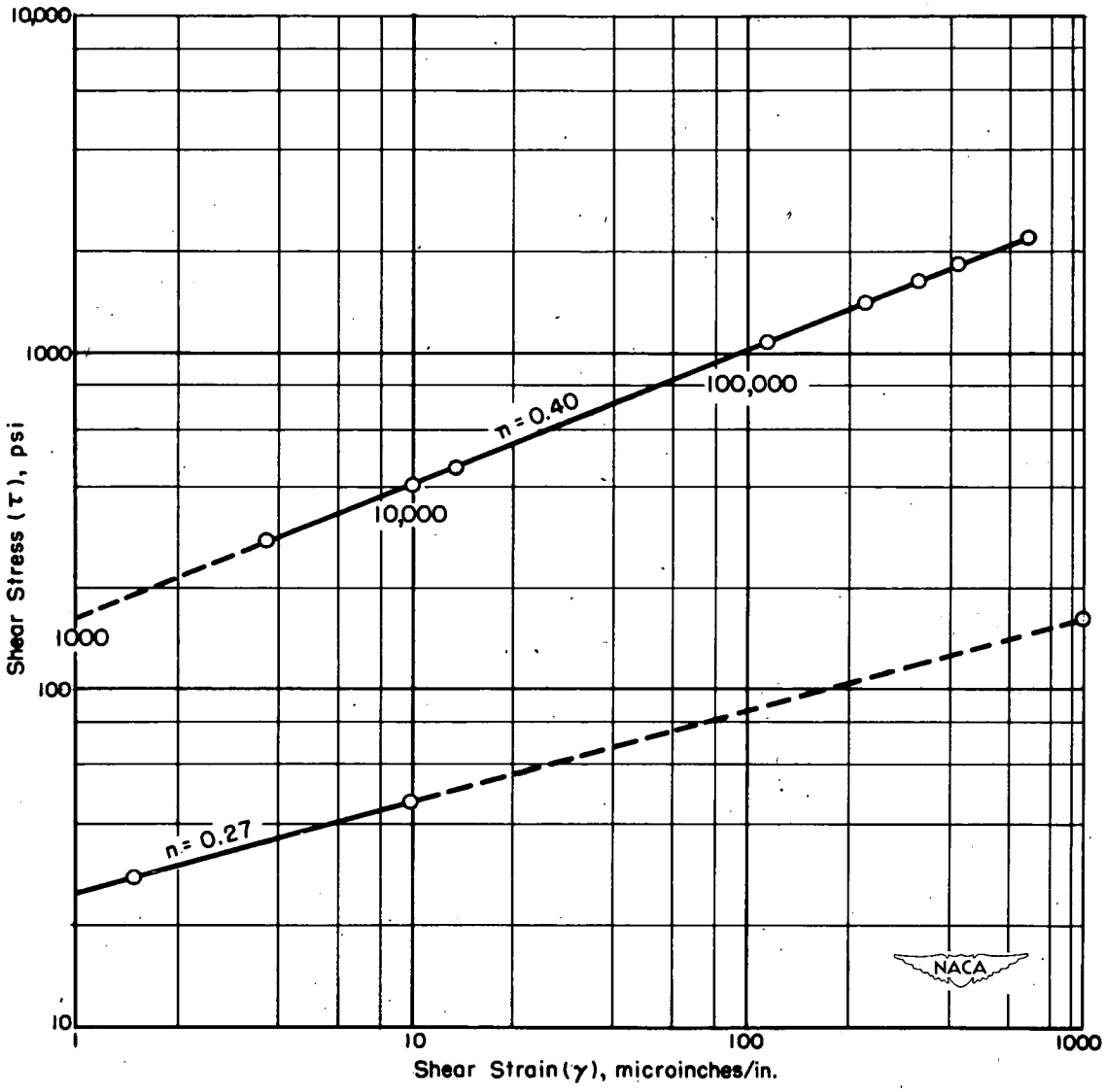

Figure 8.- Plastic shear stress-strain curves for a single crystal of aluminum (99.99+ percent pure). Crystal P-16.

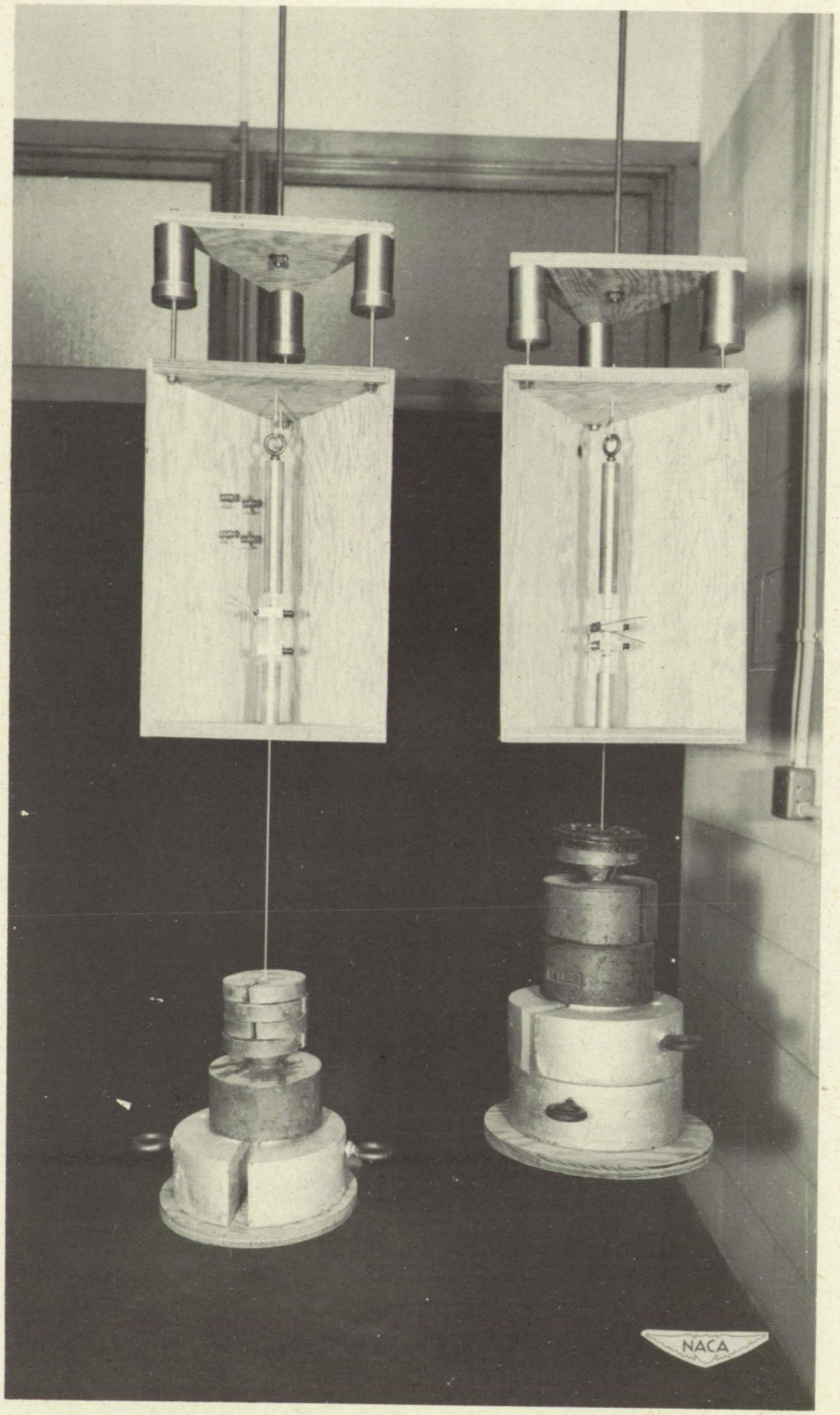

Figure 9.- Creep-testing units used for single-crystal tests.

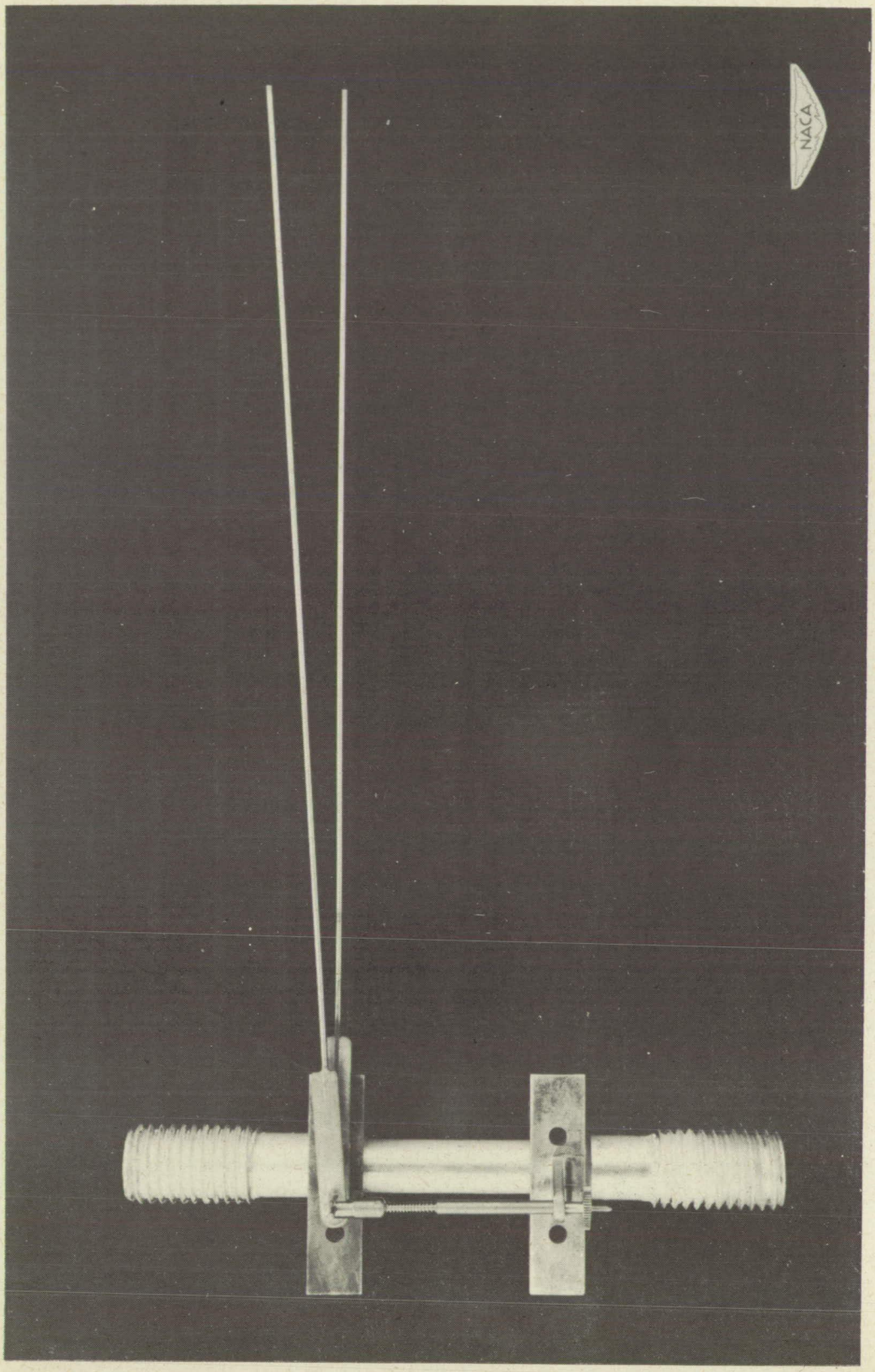

Figure 10.- Extensometer system used in creep testing of single crystals at room temperature.

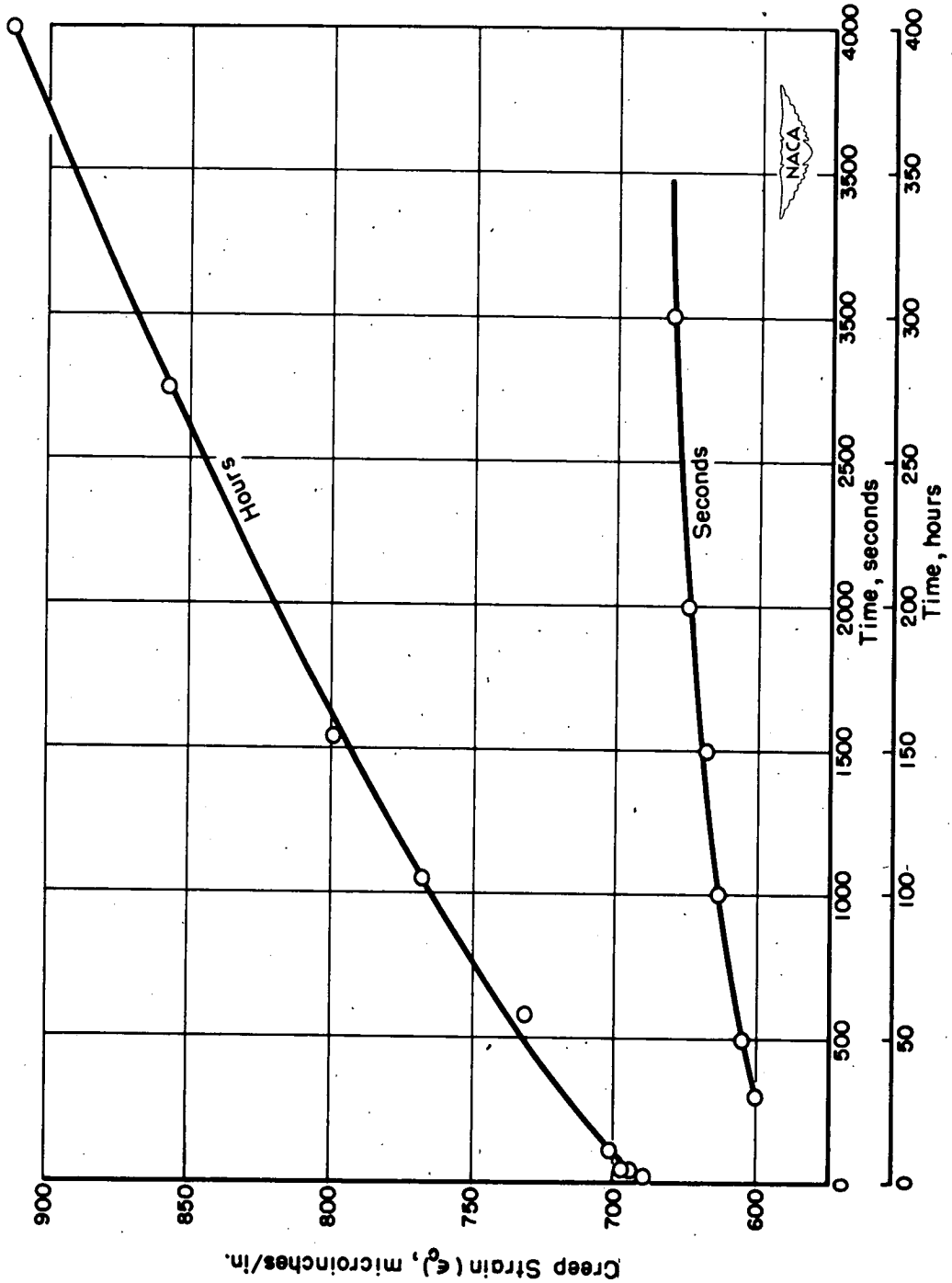

Figure 11.- Strain-time curves for crystal P-37. P/A = 462 psi; τ = 198 psi; test temperature = 36° C.

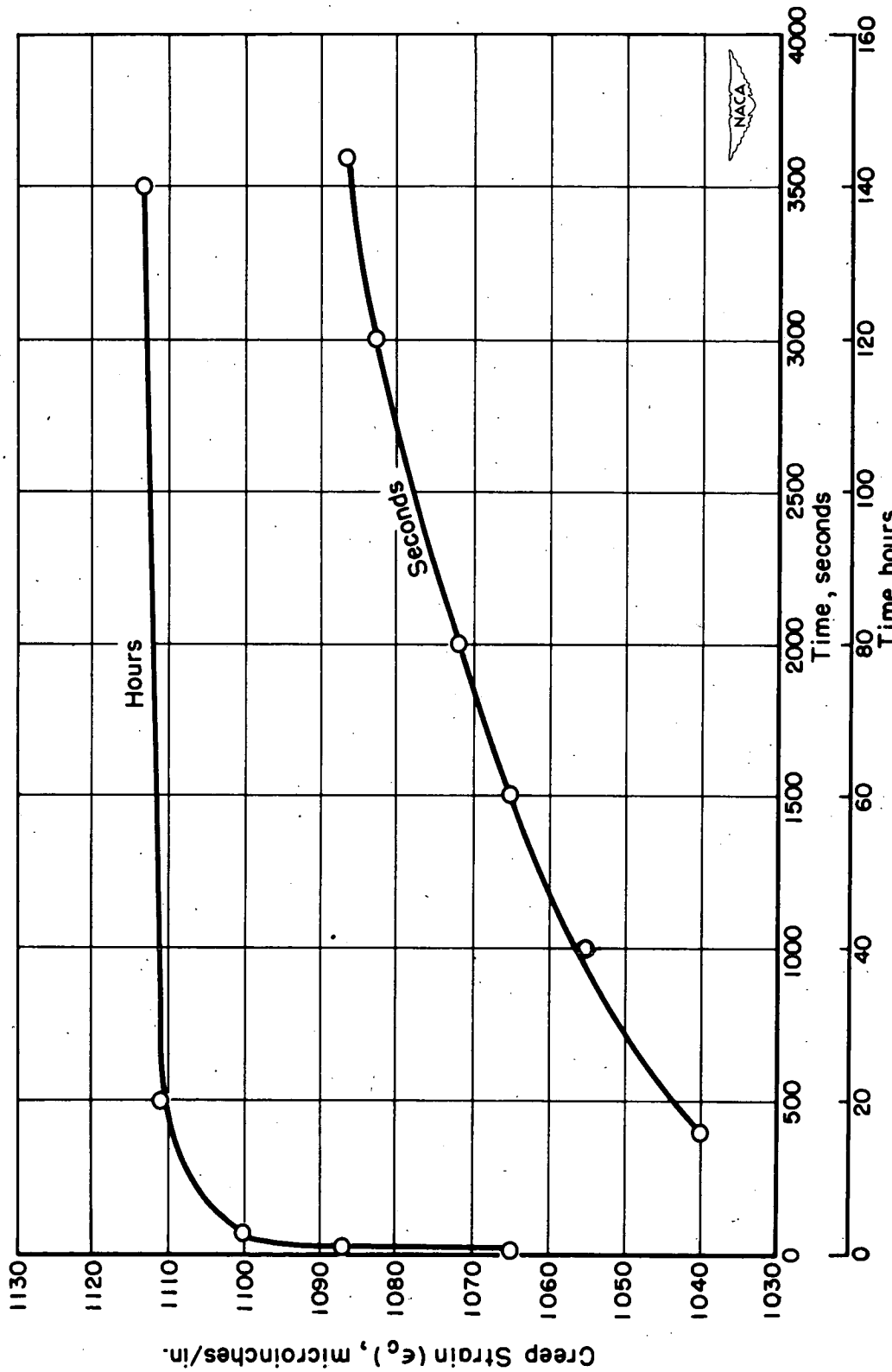

Figure 12.- Strain-time curves for crystal P-40. P/A = 528 psi; τ = 255 psi; test temperature = 36° C.

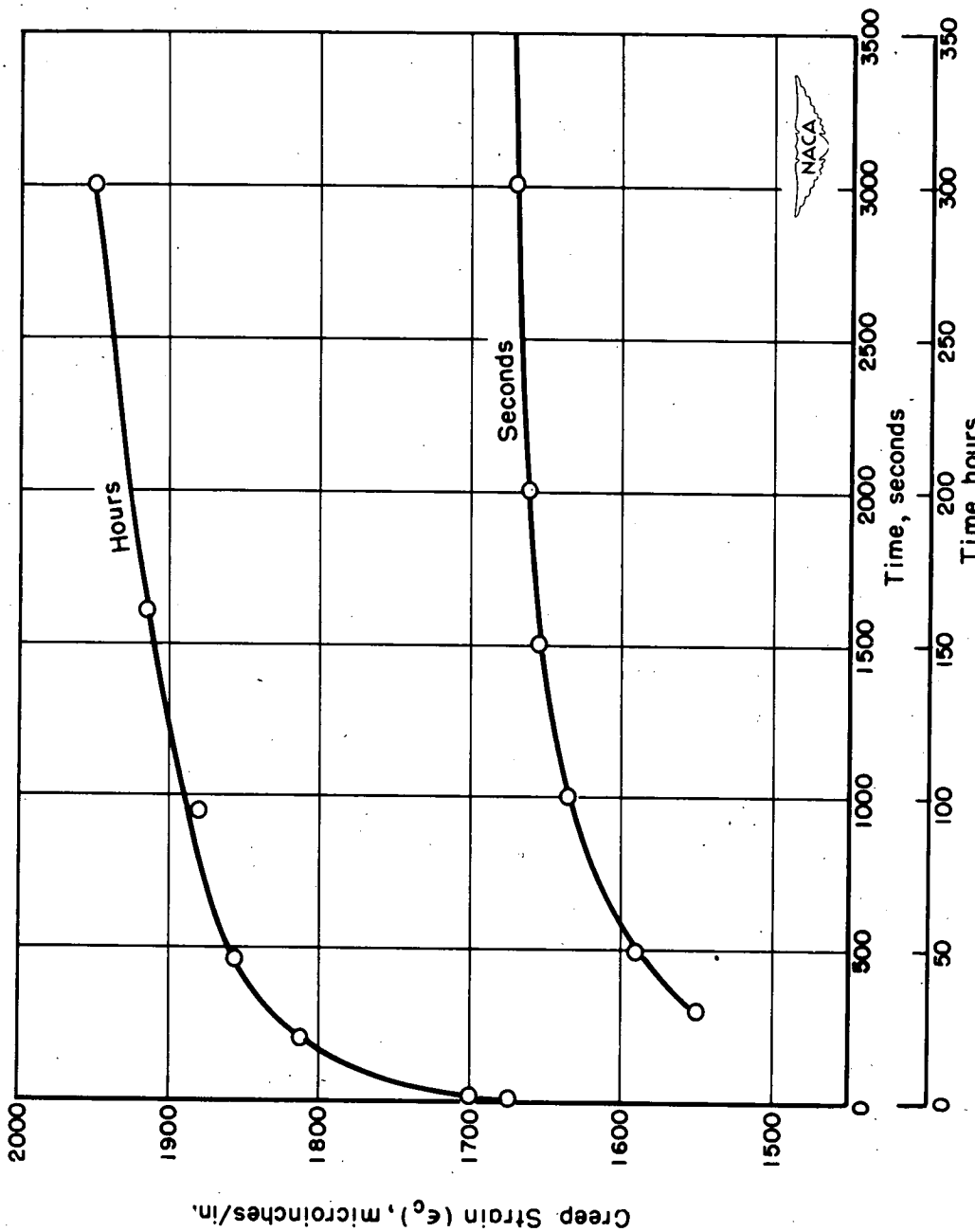

Figure 13.- Strain-time curves for crystal P-13. P/A = 645 psi; τ = 306 psi; test temperature = 36° C.

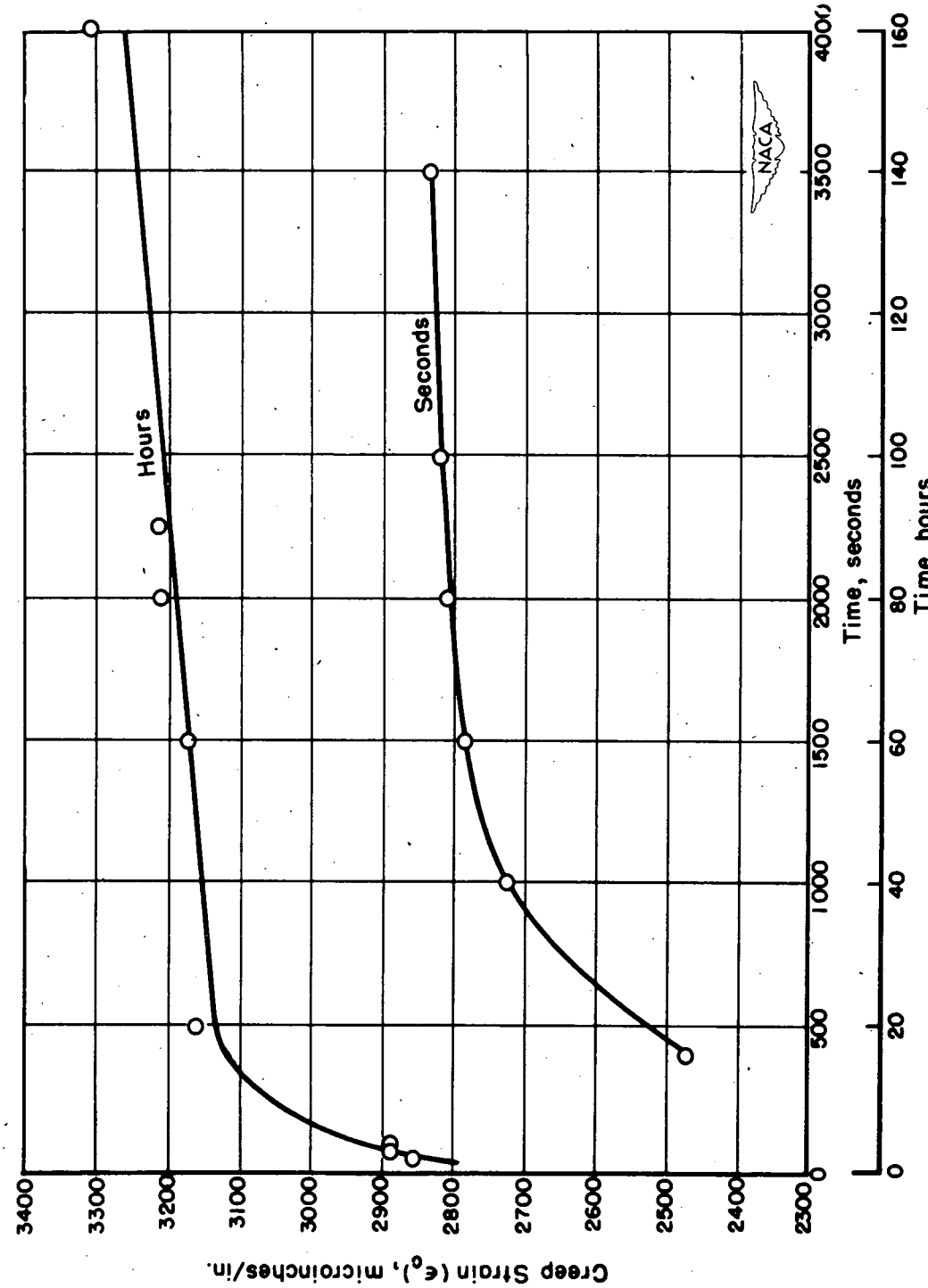

Figure 14.- Strain-time curves for crystal P-33. P/A = 764 psi; τ = 350 psi; test temperature = 36° C.

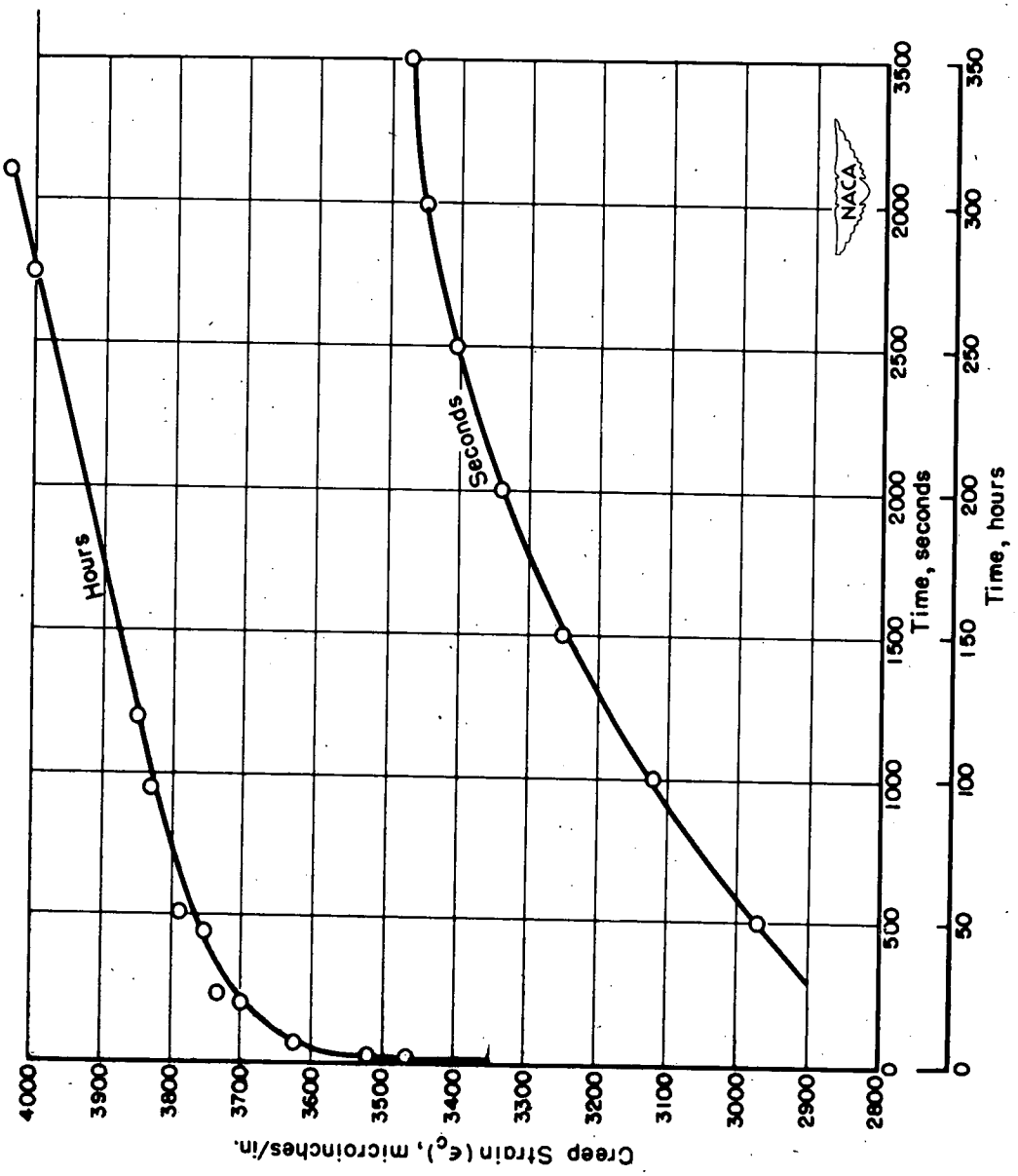

Figure 15.- Strain-time curves for crystal P-41. P/A = 805 psi; τ = 400 psi; test temperature = 36° C.

Figure 16.- Simple cubic lattice.

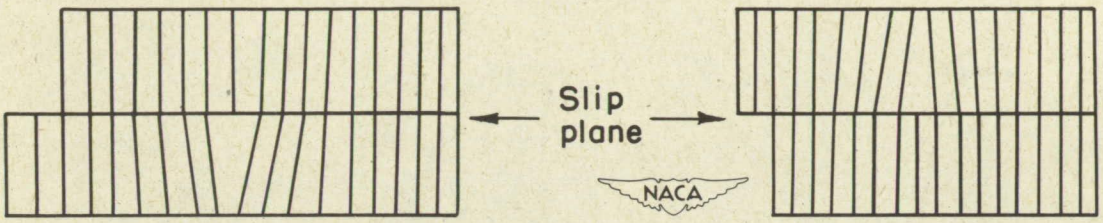

(a) Positive dislocation. (b) Negative dislocation.

Figure 17.- Edge dislocations as pictured by Taylor in reference 8.

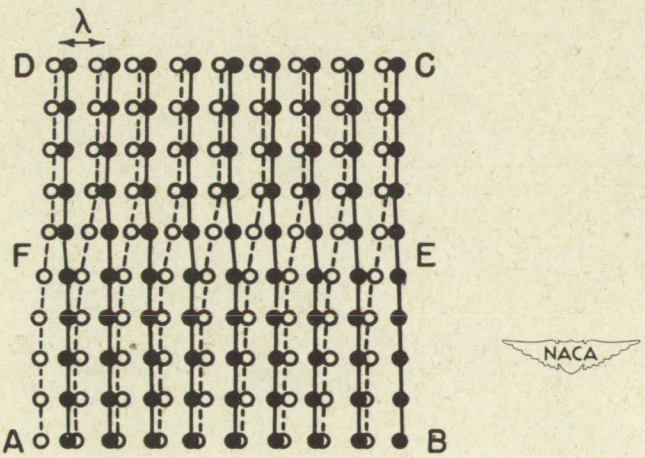

Figure 18.- Screw dislocation as pictured by Burgers in reference 9.

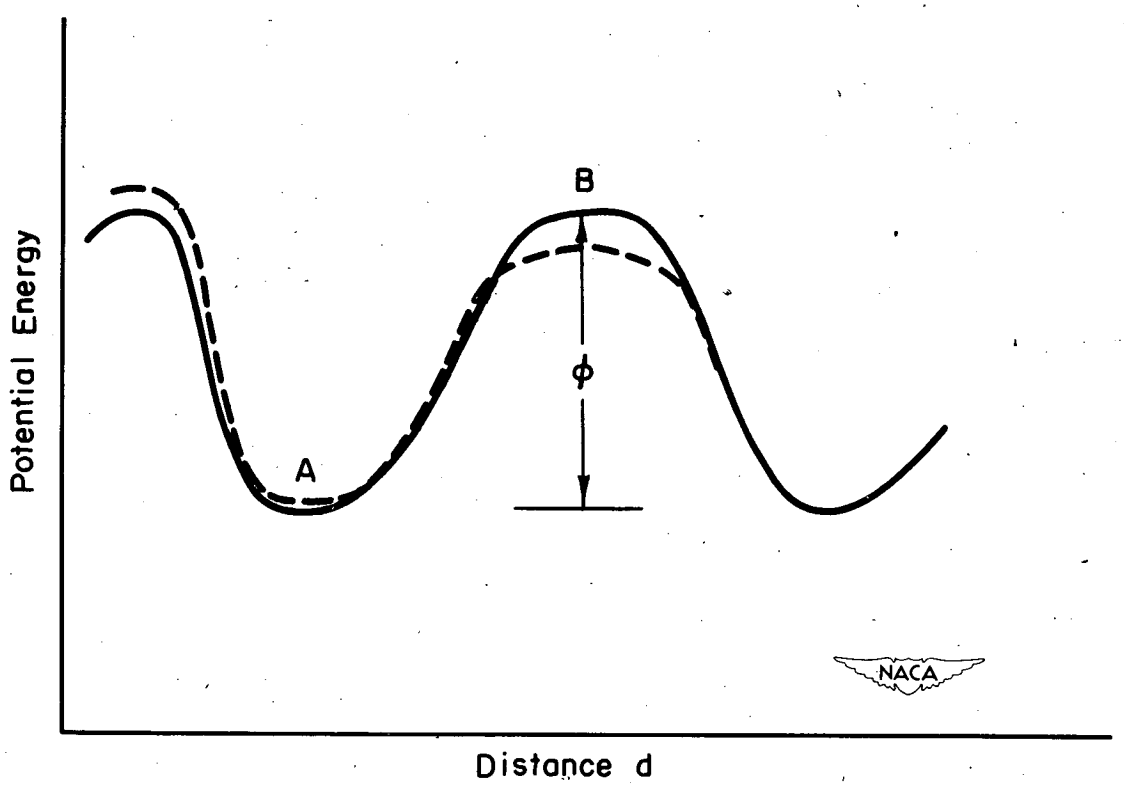

Figure 19.- Potential energy as a function of distance along an atomic plane.

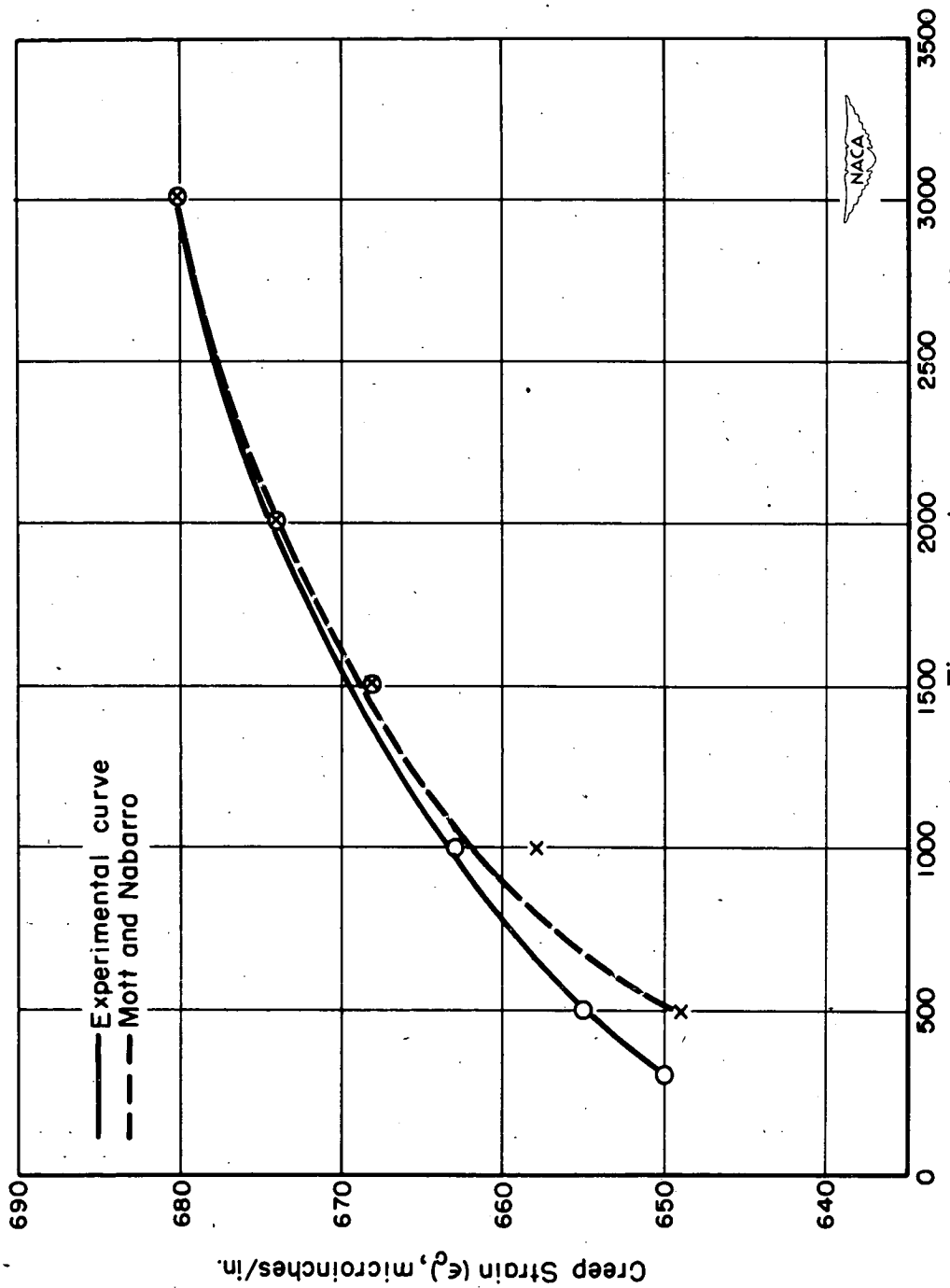

Figure 20.- Comparison of experimental curve with that predicted by Mott and Nabarro. Crystal P-37.

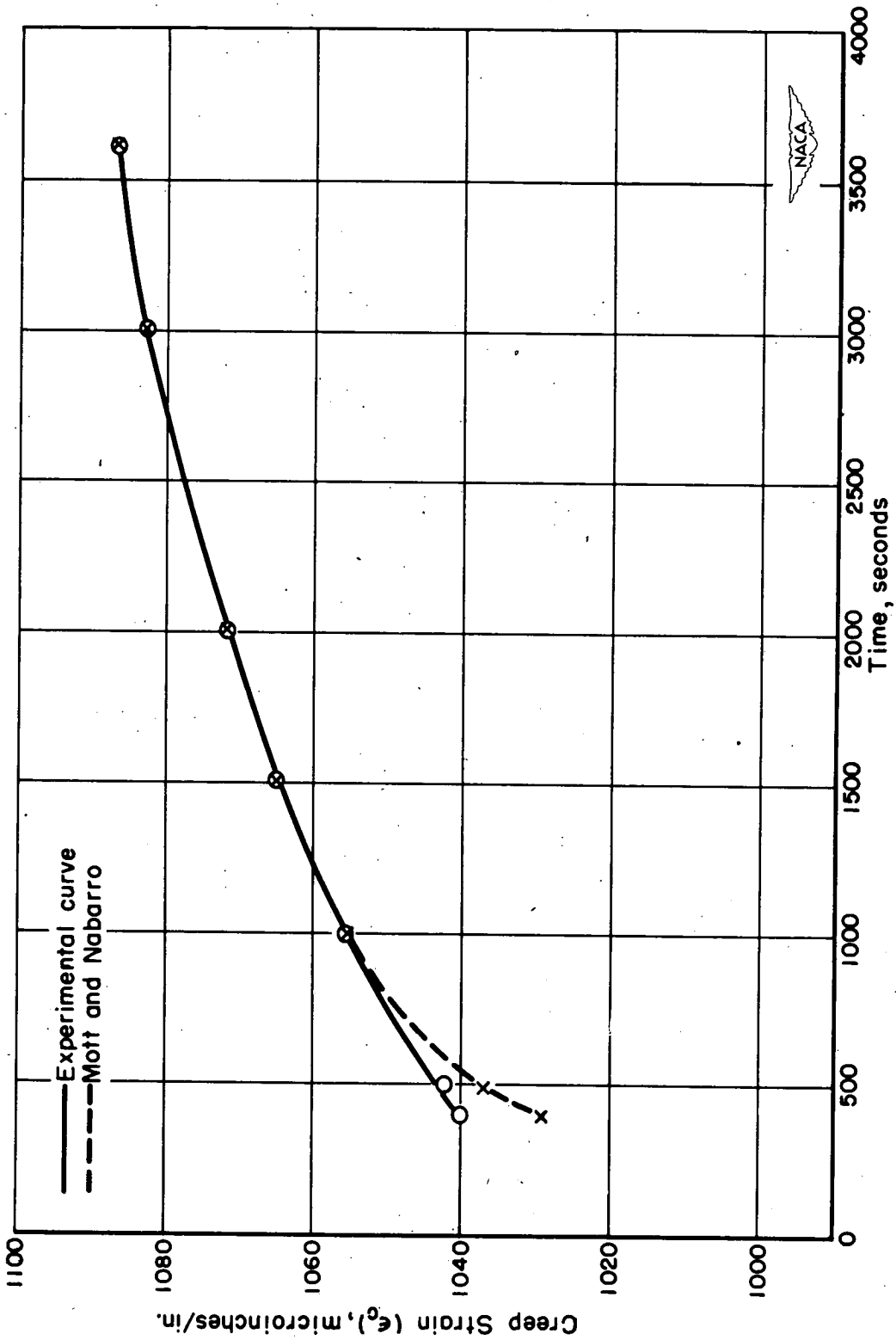

Figure 21.- Comparison of experimental curve with that predicted by Mott and Nabarro. Crystal P-40.

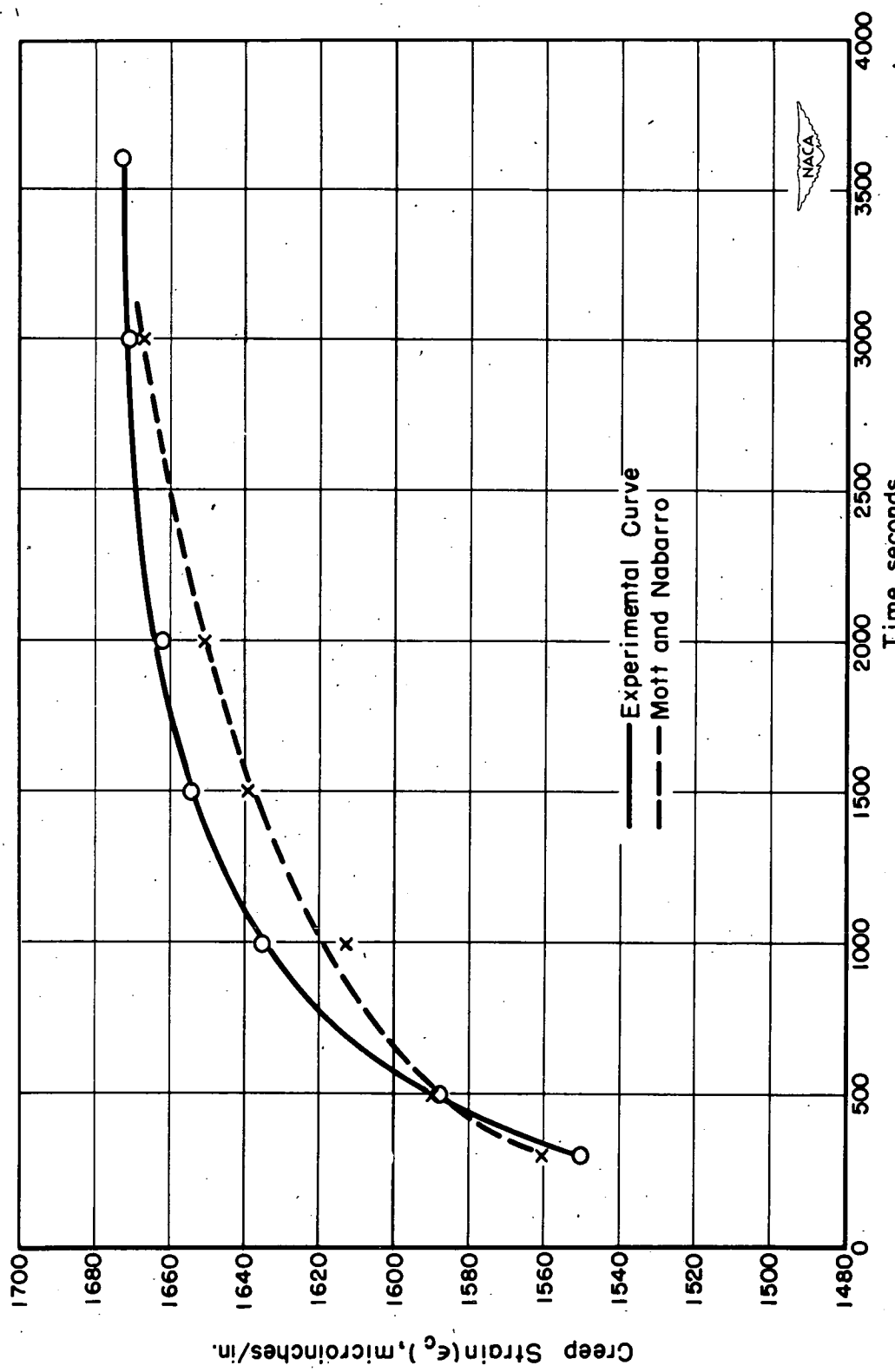

Figure 22.- Comparison of experimental curve with that predicted by Mott and Nabarro. Crystal P-13.

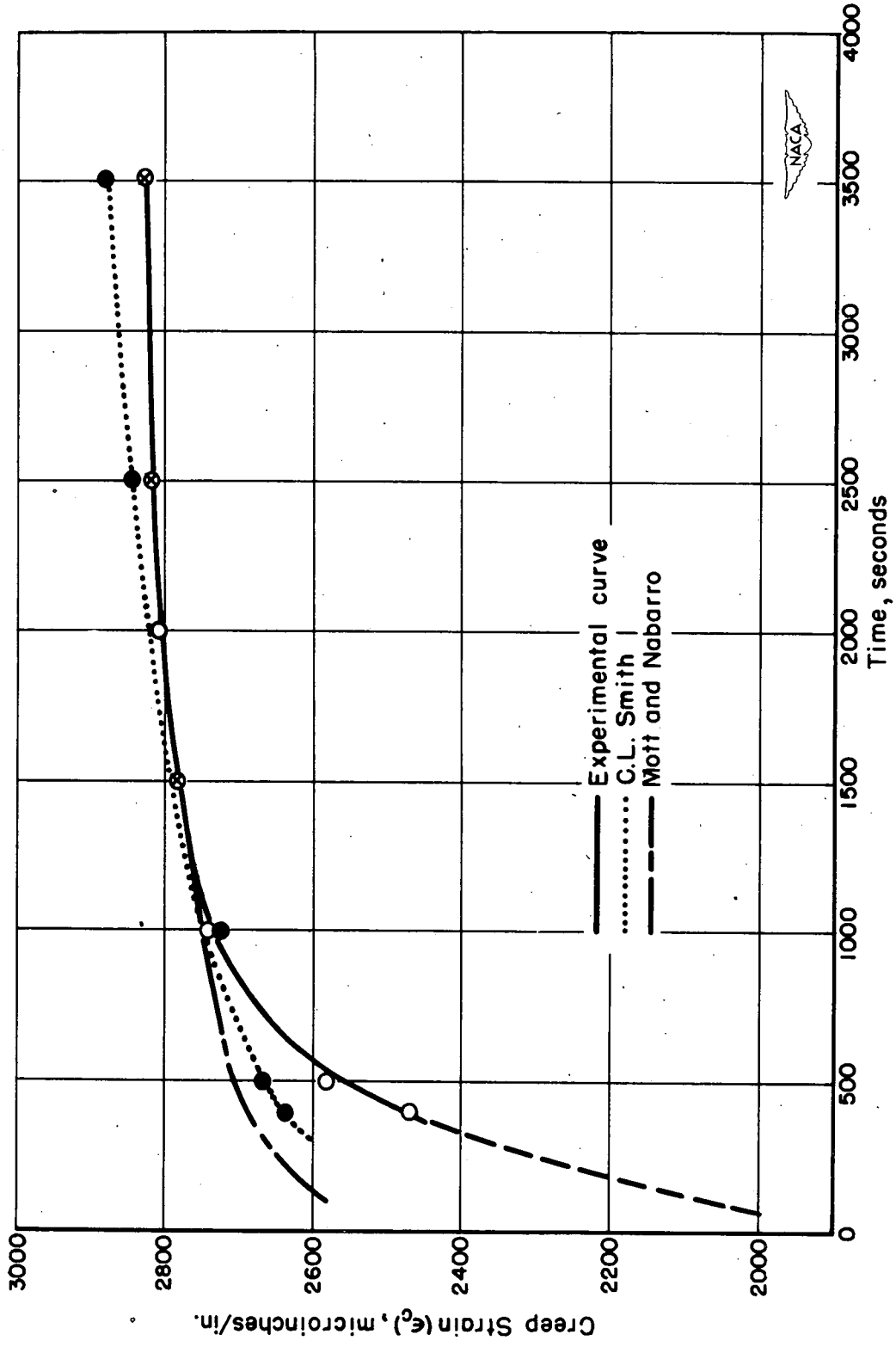

Figure 23.- Comparison of experimental curves with theoretical relations. Crystal P-33.

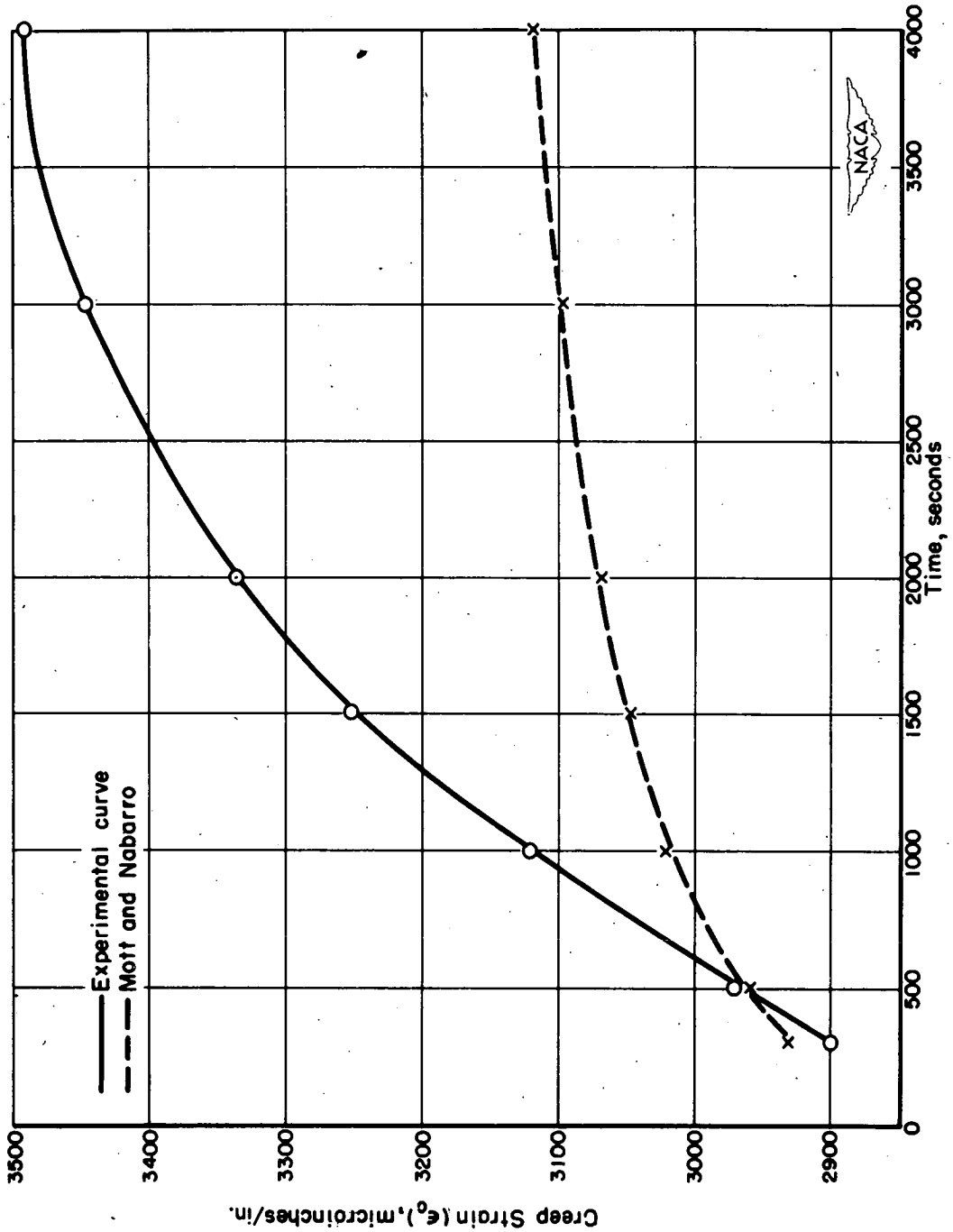

Figure 24.- Comparison of experimental curve with that predicted by Mott and Nabarro. Crystal P-41.

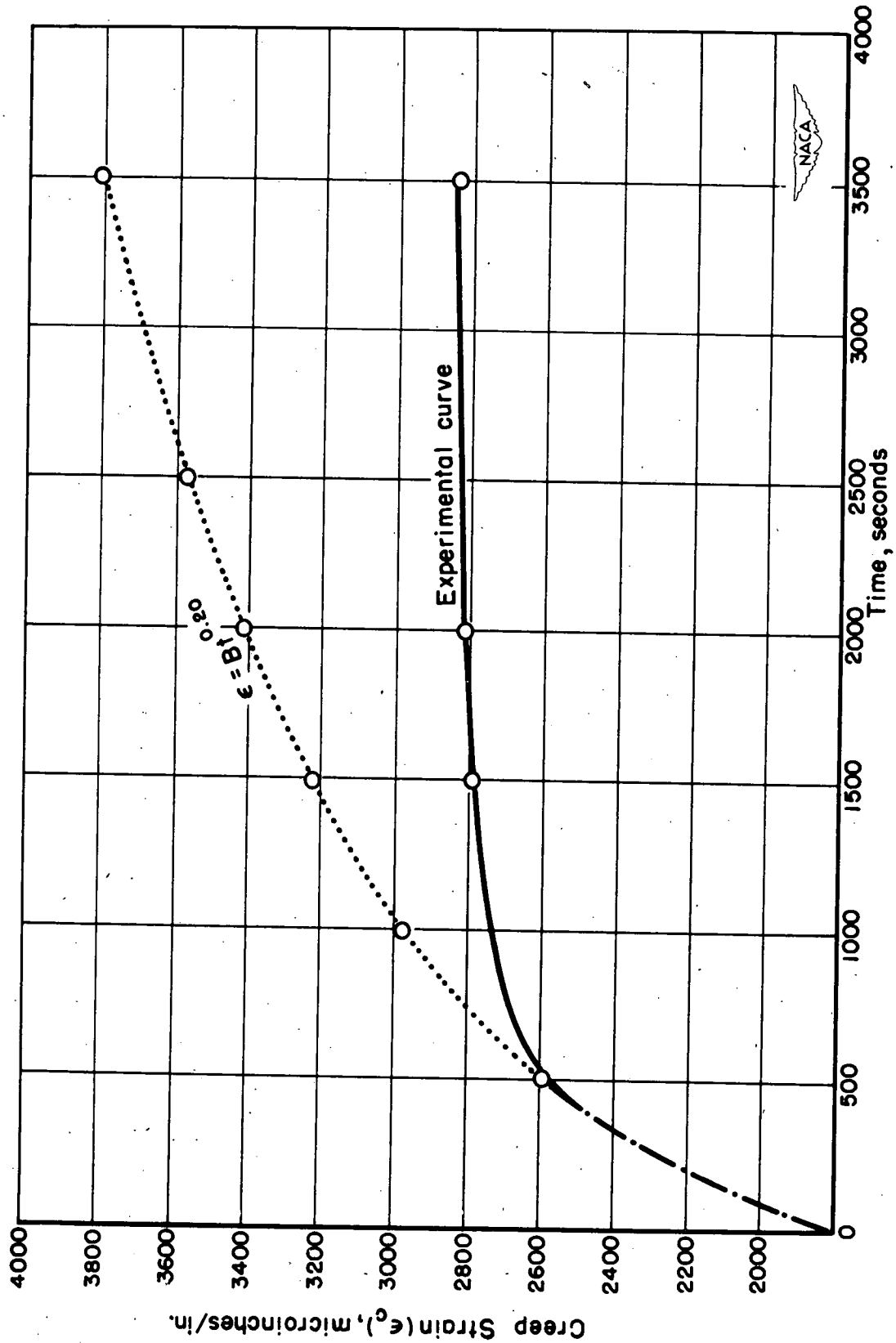

Figure 25.- Comparison of Andrade's law with experimental data.

NACA-Langley - 2-18-52 - 1000